NTNU
Norwegian University of
Science and Technology

Comparing measurements and simulations for acoustics in open-plan office spaces

Hogne Opsahl Olufsen

Master of Science in Electronics
Submission date: July 2017
Supervisor: Peter Svensson, IES

Norwegian University of Science and Technology
Department of Electronic Systems

Dedication

This thesis has given me valuable experience, it has allowed me to familiarize myself with one of the most common simulation tools for acoustics, Odeon. I have also had the opportunity to learn CATT acoustics, and the measurement program WinMLS. It has also given me the opportunity to closely relate myself to the parameters of the ISO 3382-3.

I would like to thank my supervisor Peter Svensson for steering me on the right path and his engagement in the project.

I would also like to thank my co-supervisor Daniela Toledo Helboe from COWI Oslo for valuable input and great facilitation in Oslo during the measuring period. Also thanks to Christopher Gehe and Eirik Tuftin for help with WinMLS and information about the materials in the office.

Thanks to Bård Støfringsdal, COWI Førd for valuable support and experience sharing.

I would also like to thank COWI Trondheim, for letting me use Odeon and providing a desk for me in an open-plan office. That allowed me to experience pros and cons related to my thesis work.

Summary

This report is the result of a master thesis at the Norwegian University of Science and Technology (NTNU). The ISO 3382-3 [2] describes the measurement procedure of room acoustical parameters in an open-plan office. The aim was to investigate how well these parameters could be simulated, by comparing measured and simulated values. A special study of diffraction has also been conducted, indicating that Odeon strongly underestimates diffraction.

Measurements and simulations of the reverberation time, RT, and the ISO 3382-3 parameters have been done in two Zones of the COWI main office in Oslo. The parameters are the the A-weighted SPL based parameters ($D_{2,s}$, $L_{p,A,S,4m}$, $L_{p,A,B}$) and the STI based parameters (STI in nearest workstation, r_d , r_p). The absorption and scattering coefficient of the materials in the simulation model were adjusted such that the simulated RT was similar to the measured RT. Then the ISO 3382-3 parameters were estimated from the simulation.

The measured and simulated ISO 3382-3 parameters were quite similar for one Zone in the office, but not for the other Zone.

Preface

Open-plan offices spaces have some contradicting requirements. The employees need to be able to hear each other when working as teams, but not be distracted by others when working alone, especially when solving concentrations demanding tasks. The noise in open-plan offices consists of many different sounds, such as speech, laughter, ring tones, impact noise, traffic and other outdoor noise, ventilation and air-conditioning noise, printers and copy machines. The most annoying factor for concentration and cognitively demanding tasks is speech. A large STI can lead to distracted employees and a loss in productivity up to as much as 7%, Hongisto [19]. Hence, investment to improve the acoustics in an open-plan office space can lead to positive long term effects, such as more satisfied employees and higher productivity.

The goal is to simulate and measure the ISO 3382-3 [2] parameters in an open-plan office, using the geometrical acoustic software Odeon. The objective is to compare measured parameter values to simulated parameter values, and too evaluate if the parameters correlate with one another for the measurements and for the simulations. A sub task is to verify if simulation tools like CATT and Odeon are suitable for looking at nuances in the ISO 3382-3 parameters. This should be done by implementing a special study of edge diffraction.

Simulation is an important tool when designing open-plan offices, but what is the quality of the simulations? The quality can be considered based on the resulting values of the ISO 3382-3:2012 parameters. The parameters can be separated into two categories;

- The A-weighted SPL based parameters ($D_{2,s}$, $L_{p,A,S,4m}$, $L_{p,A,B}$)
- The STI based parameters (STI in nearest workstation, r_d , r_p)

Open-plan offices are usually quite large and many have relatively low ceilings, there are also often screen and/or other object obscuring the path between the employees. Open-plan offices are seldom a diffuse filed case. Therefore, two widely discussed issues when it comes to simulation in general and of open-plan offices in particular, are the accuracy of the edge diffraction and the angle dependent absorption. Not all acoustical simulation tools include angle dependent absorption, but rather assume diffuse incoming waves. There has not been conducted a study on the angle dependent absorption, but this would be a natural next step.

Table of Contents

List of Tables

List of Figures

Abbreviations

STI	=	Speech transmission index
SPL	=	Sound pressure level
SNR	=	Signal to noise ratio
ML	=	Measurement line
BGN	=	back ground noise level
FR	=	Frequency response
IR	=	Impulse response
NC	=	Noise Criterion
S-R	=	Source to receiver
DP	=	Decrease in performance
SII	=	Speech intelligibility index
S_n	=	Source position n
R_n	=	Receiver position n

Chapter 1

Introduction

Chapter 2 provides a literature review with reference to external studies on the use of open-plan offices, while reference to theory and software used in this work is given in the text when applicable. Chapter 3 contains theory on the parameters that are investigated in the study. Chapter 4 explains the methods used for measuring and simulating of an open-plan office. Chapter 5 shows the results along with discussion of the results. Chapter 6 presents a special study on diffraction analyses with various software model, and gives an independent description of methods, results, discussion and conclusion. Chapter 7 contains a general discussion of the results along with sources of uncertainty. A general conclusion of the work is presented in Chapter 8.

Chapter 2

Literature Review

This chapter deals with and refers to external studies on the use of open-plan offices.

The open-plan office structure was originally designed for teamwork and knowledge exchange, but today it is used more widely for all types of offices. The trend is associated with economic and architectural advantages and easier knowledge exchange and communication between employees. However, filed studies, such as Haapakangas et al. [15] and Danielsson [12], show discontent with the acoustic environment in open-plan offices.

One of the largest disturbances in a open-plan offices is the sound environment. The noise in an open-office is composed of multiple sounds such as speech, laughter, ring tones, typing on keyboards, printers, coffeemakers, outdoor and ventilation noise and much more. When a worker are doing concentration demanding work, understandable speech is very distracting and will often result in lower productivity. In these situation, it is desirable with a low speech intelligibility. The effects of irrelevant speech on the productivity has been studied using psychological experiments Haka et al. [16].

Figure 2.1 is a model showing the decrease in performance versus STI. This model is taken from Hongisto [19]. The predictive model is part of Hongisto's earlier work, Hongisto [18]. It is based on experimental data from the following three studies. Venetjoki et al. [28], whom studied the effect of speech on proof-reading performance. Ellermeier and Hellbrück [14], whom studied the recall of digits in different SNR of speech. And Kaarlela-Tuomaala et al. [20], whom studied the effects of office noise on office workers using questionnaires. From the model in Figure 2.1 we see that a reduction from an STI of 0.2 to 0.6 gives a decrease in productivity, DP, of roughly 7%.

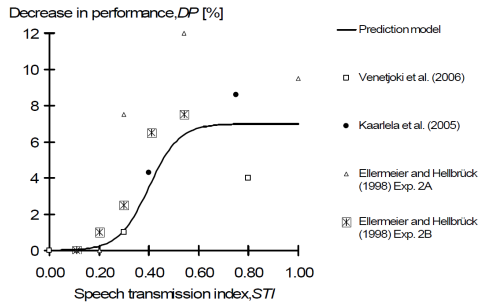

Figure 2. Work performance decreases with increasing speech intelligibility in offices.

Figure 2.1: DP versus STI, Hongisto [19].

This predictive model was used when deciding the STI for the distraction distance, r_d, and privacy distance, r_p in the ISO 3382-3 [2]. The distraction distance was set to the distance when the STI is 0.5, since the decrease in work performance rapidly descents when the STI gets below 0.5. The privacy distance was set to 0.2 as there is almost no decrease in work performance when the STI gets below 0.2.

Improving the acoustics of open-plan offices can therefore give large economic effects as it can increase the productivity of the employees. This is also largely dependent on the intended work in the office. Papers such as Bradley et al. [7], show the effect altering different room parameters has on the SII. Some of the room parameters are the absorption of the ceiling, floor and screen, the height of the ceiling and screens. The SII is another parameter that describes the speech intelligibility, similar to the STI.

Chapter 3

Theory

The theory section describes the ISO 3382-3 parameters used to rate the ”worst case” acoustic conditions of an open-plan office. One speaker gives worst case, since multiple speakers give a masking effect for the STI. The ISO 3382-3 [2] parameters are divided into two groups, i.e. the A-weighed SPL based parameters and the STI based parameters. Table 3.4 shows the classification from A to D of the ISO 3382-3 [2] parameters and reverberation time. A is the best case and D the worst. Further, diffraction, scattering, linear regression and how correlation is estimated defined. At the end there is a small discussion to link the parameters.

3.1 A-weighted sound pressure level based parameters

3.1.1 A-weight and Sound pressure level of normal speech

The A-weight for each 1/1 octave band from $125Hz - 8kHz$ is denoted as A_i and given in Table 3.1. The sound pressure level of normal speech at 1m from an omni directional source is given in Table 3.1, ISO 3382-3 [2].

Table 3.1: A-weight and Sound pressure level of normal speech at 1m from an omni directional source, ISO 3382-3 [2].

Freq [Hz]	**125**	**250**	**500**	**1000**	**2000**	**4000**	**8000**
A_i	-16.1	-8.6	-3.2	0.0	1.2	1.0	-1.1
L_{p,S,1m,i}	49.9	54.3	58.0	52.0	44.8	38.8	33.5

This results in a total A-weighted sound pressure level of normal speech at 1m from an omni directional source of $57.4dB(A)$.

3.1.2 Distance attenuation of speech, $D_{2,S}$

$D_{2,S}$ is a measure of the spatial attenuation of the A-weighted sound pressure level of speech per doubling of the source to receiver distance, ISO 3382-3 [2]. To estimate this parameter, a couple of other estimations have to be done. First $D_{n,i}$ has to be estimated, it is the dampening in measurement point n for the 1/1 - octave band from $125Hz - 8kHz$, denoted i.

$$D_{n,i} = L_{p,Ls,1m,i} - L_{p,Ls,n,i} \tag{3.1}$$

$L_{p,Ls,1m,i}$ is the measured sound pressure level at 1m in free field, and $L_{p,Ls,n,i}$ is the measured sound pressure level at measurement point n. $L_{p,Ls,1m,i}$ is obtained by using a rectangular filter on the measured signal at 1m to remove reflections from the impulse response. Thereafter, the sound pressure level of normal speech in measurement point n, $L_{p,S,n,i}$, is estimated.

$$L_{p,S,n,i} = L_{p,S,1m,i} - D_{n,i} \tag{3.2}$$

where $L_{p,S,1m,i}$ is the sound pressure level of speech at $1m$ from a omni directional source, given in Table 3.1, and $D_{n,i}$ is the dampening in measurement point n and i denotes the 1/1 - octave band from $125Hz - 8kHz$. From this, $L_{p,A,S,n}$, the A-weighted speech level in measurement point n, can be estimated from.

$$L_{p,A,S,n} = 10lg(\sum_{n=1}^{7} 10^{\frac{L_{p,S,n,i}+A_i}{10}}) \tag{3.3}$$

where $L_{p,S,n,i}$ is the sound pressure level of normal speech in measurement point n, estimated from Equation 3.2, and A_i is the correction for A-weighting shown in Table 3.1. Finally, $D_{2,S}$, can be estimated as.

$$D_{2,S} = -lg(2)\frac{\sum_{n=1}^{N}[L_{p,A,S,n}lg(\frac{r_n}{r_0})] - \sum_{n=1}^{N} L_{p,A,S,n} \sum_{n=1}^{N} lg(\frac{r_n}{r_0})}{N\sum_{n=1}^{N}[lg(\frac{r_n}{r_0})]^2 - [\sum_{n=1}^{N} lg(\frac{r_n}{r_0})]^2} \tag{3.4}$$

where n is an index for a measurement point, N is the total number of measurement points, r_n is the source receiver distance to measurement point n, r_0 is the reference distance of $1m$, $L_{p,A,S,n}$ is the A-weighted speech level in measurement point n.

3.1.3 A-weighted sound pressure level of speech at 4m distance, $L_{p,A,S,4m}$

A-weighted sound pressure level of speech at 4m distance, $L_{p,A,S,4m}$, is as the name describes, the A-weighted sound pressure level of speech at $4,0m$ distance from the source. It can be estimated using a linear regression line of the the A-weighted speech level in measurement point n, $L_{p,A,S,n}$, and the source receiver distance at measurement position n.

3.1.4 Background noise level, $L_{p,B}$ and $L_{p,B,n}$

$L_{p,B,n}$, is the mean background noise level in 1/1 octave band from $125Hz - 8kHz$ at each measurement position n. It is measured at each workstation (desk) (see Chapter 4), without people being present, 3382-3 [2]. $L_{p,B}$, is the mean of all the background noise measurements and is given in 1/1 octave band values from $125Hz - 8kHz$.

3.2 Speech transmission index, STI

The STI is a physical measurement that quantifies the quality of transmitted speech with regards to speech intelligibility. The result is a number from 0 to 1, where 1 means perfect transmission and 0 means no speech can be recognized, ISO 3382-3 [2]. Table 3.2 shows the speech intelligibility and speech privacy for different STI values.

Table 3.2: STI, Speech intelligibility and speech privacy, [8]

STI	Speech intelligibility	Speech privacy
$0.00 - 0.05$	very bad	confidential
$0.05 - 0.20$	bad	good
$0.20 - 0.40$	poor	reasonable
$0.40 - 0.60$	fair	poor
$0.60 - 0.75$	good	bad
$0.75 - 0.99$	excellent	very bad

3.2.1 Distraction distance, r_d

The distraction distance, r_d, is the distance from the speaker at which the STI falls below $0,50$. For distances above the distraction distance, concentration and the experience of un-distractedness quickly improves. Figure 11 shows an example of how the distraction distance is estimated.

3.2.2 Privacy distance, r_p

The privacy distance, r_p, is the distance from the speaker at which the STI falls below $0,20$. Figure 11 shows an example of how the privacy distance is estimated.

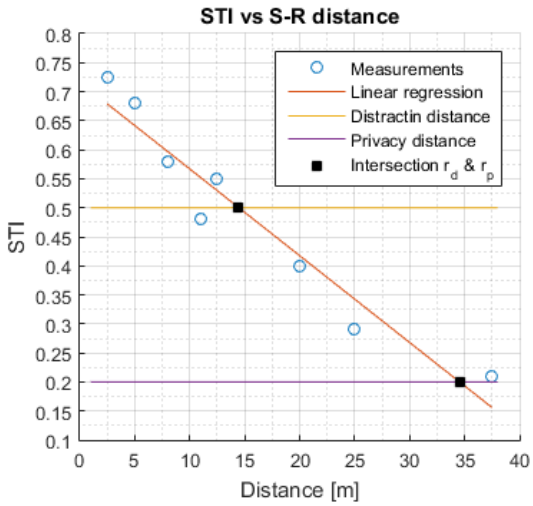

Figure 3.1: STI versus source to receiver (S-R) distance, with lines for distraction and privacy distances.

3.3 Linear regression

Linear regression analysis is used to fit the variability in measured data. The linear regression line is a function on the form $\hat{y} = b_0 x + b_1$, that describes the predicted development of the dependent variable y. x is the independent variable and b_1 is a constant that denotes the $\hat{y}$ intercept of the regression line. The slope of the regression line is given as b_0.

The deviation from the regression line is called the residual and is shown i Figure 3.2. The method of least squares is one of the most common method for minimizing the sum of the squares of the residuals. Probability & statistics [30], was used as reference literature for linear regression.

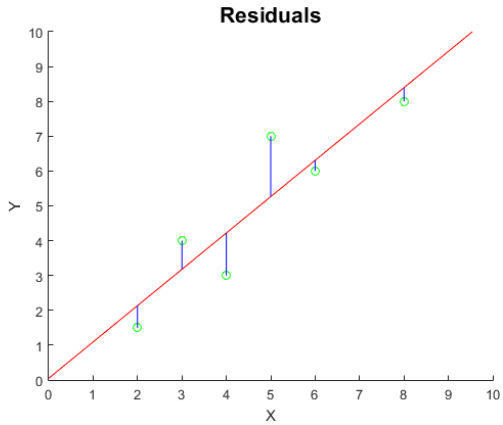

Figure 3.2: Plot of residuals.

Using this method, the slope of the regression line, b_0, is obtained from the Equation 3.5, Probability & Statistics [30].

$$b_0 = \frac{\sum_{n=1}^{N}(x_n - \bar{x})(y_n - \bar{y})}{\sum_{n=1}^{N}(x_n - \bar{x})^2} \tag{3.5}$$

where x_n denotes the independent data sett, $\bar{x}$ denotes the mean of the independent data set. y_n denotes the dependent data sett, $\bar{y}$ denotes the mean of the dependent data sett. And the interception b_1, is obtained from Equation 3.6, Probability & Statistics [30].

$$b_1 = \bar{y} - a\bar{x} \tag{3.6}$$

3.3.1 Diffraction

Diffraction is bending of wave due to a barrier, object or a small opening. When a sound wave encounters an a obstacle, some of the sound is reflected, some of it continues through and some is diffracted around the obstacle. If the wavelength of the sound wave is larger than the obstacle, the wave is diffracted around it. Sound waves with longer wavelengths are bent more than waves with shorter wavelengths. When wavelengths are smaller than the obstacle, the wave are reflected or absorbed and diffraction barely happens, the Physics Classroom[10].

Figure 3.3 shows the fundamentals of diffraction.

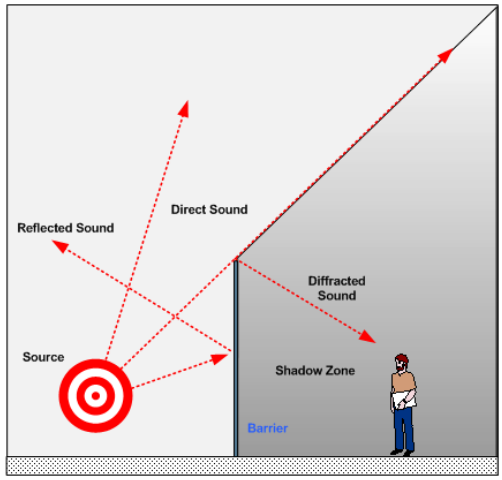

Figure 3.3: Illustration of diffraction over a wall, the Physics Classroom[10].

3.4 Scattering coefficient

The scattering coefficient is a measure of the amount of sound scattered in a different direction from the secular reflection and it plays an important role particularly in the late response. The scattering coefficient is defined as one minus the ratio between the specularly reflected acoustic energy and the total reflected acoustic energy. When measured in an approximate diffuse sound field it is called the random-incidence scattering coefficient with the symbol s and values between 0 and 1. The scattering coefficient describes the degree of scattering due to the roughness or irregularity of a surface. The scattering due to diffraction from the edges is not included in Odeon [9].

Instead of specifying the scattering coefficient for each octave band, Odeon uses one coefficient for the scattering, and estimates values it for the other octave bands using interpolation or extrapolation. Figure 3.4 below is taken from the Odeon manual [9], and shows some estimation curves.

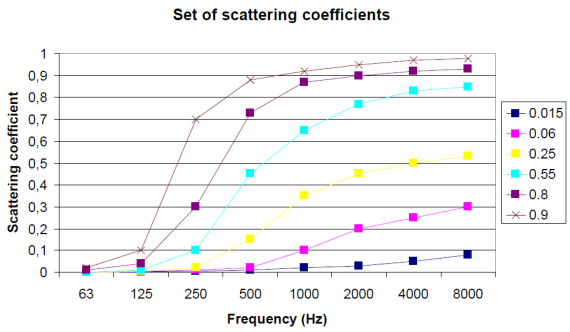

Figure 3.4: Surface scattering, Odeon User's Manual[9].

The Odeon Users's Manual [9] also has a table with some recommended scattering coefficients for different surfaces, shown in the Table 3.3

Table 3.3: Scattering coefficient at mid-frequency $(707Hz)$, Odeon User's Manual [9]

Material	**Scattering coefficient at mid-frequency**
Audience area	0.6 – 0.7
Rough building structures,	0.3 – 0.5 m deep 0.4 – 0.5
Bookshelf, with some books	0.3
Brickwork with open joints	0.1 – 0.2
Brickwork, filled joints but not plastered	0.05 – 0.1
Smooth surfaces, general	0.02 – 0.05
Smooth painted concrete	0.005 – 0.02

3.5 NS 8175

Table 3.4 shows different requirements of the NS 8175 standard [6]. The label table refers to the tables in the standard where the data have been retrieved from. A common requirement for the back ground noise level, BGN, in offices is Class C.

Table 3.4: Information from NS 8175 [6].

Table	**Type space**	**Measure**	**Class A**	**Class B**	**Class C**	**Class D**
34	**Office**	$L_{p,AT}$	28	28	33	38
		$L_{p,AF,max}$	30	30	35	40
33	**Open-plan office**	T_h	0.11*h	0.13*h	0.16*h	0.20*h
E.1	**Open-plan office**	$DL_{2,s}$	>= 11	>=9	>=7	<7
		$L_{p,A,S,4m}$	<=46	<=49	<=52	>52
		r_d	>=5	>=8	>=11	<11
		STI	0.1	0.15	0.2	0.3
		STI	0.8	0.7	0.6	0.5

3.6 Correlation

Correlation analysis attempts to measure the strength of the relationship between two variables and portray it as a single number value, the correlation coefficient. The correlation coefficient has a value between $+1$ and -1, that indicates total positive and negative linear correlation. A doubling of the coefficient does not necessarily indicate that the relationship is twice as good, only that it is better, Probability & Statistics [30].

Figure 3.5 show examples of negative, zero and positive linear correlation.

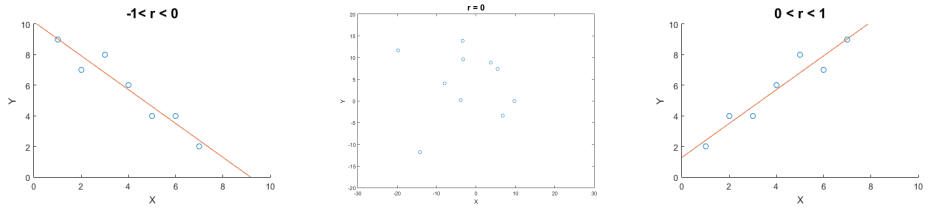

(a) Negative linear correlation **(b)** Zero linear correlation **(c)** Positive linear correlation

Figure 3.5: Linear correlation

One estimate of the correlation coefficient is r, the Pearson product-moment correlation coefficient, or simply the sample correlation coefficient. It is given by the Equation 3.7.

$$r = \frac{S_{xy}}{\sqrt{S_{xx}S_{yy}}} = \frac{\sum_{n=1}^{N}(x_n - \bar{x})(y_n - \bar{y})}{\sqrt{\sum_{n=1}^{N}(x_n - \bar{x})^2}\sqrt{\sum_{n=1}^{N}(y_n - \bar{y})^2}} \tag{3.7}$$

Where y_n represent the dependent data set and $\bar{y}$ represents the mean value of that data set. x_n represent the independent data set and $\bar{x}$ represents the mean value of that data set, Probability & Statistics [30].

3.7 Application of theory

The choice of scattering coefficient will have a large impact on the reverberation time, RT. For the frequencies above 2kHz, the air absorption will be the most dominant absorption. From Figure 3.3 we see that scattering is much higher for the high frequencies. A high scattering at the high frequencies will result in lower RT, and vice versa. The A-weighted SPL of speech parameters are independent of the BGN, while the STI based parameters are highly dependent on it. A study on the correlation between the A-weighted SPL of speech, the STI based parameters, the A-weighted SPL of speech and STI parameters and between the STI based parameters and the BGN is of interest. Correlation between the A-weighted SPL of speech and the BGN is of no interest as they are independent.

A higher BGN will give a lower STI. Masking systems are very uncommon in Norway, and whether or not they are to be described as an aid to the acoustics or part of the background noise in the office has not yet been decided. Studies such as Bradley [5] have concluded that a preferable A-weighted sound pressure level for the masking sound is around 45 dBA and should not exceed 48 dBA.

The measurement report for ISO 3382-3 [2], should include a graph of the $L_{p,B,n}$ is along with $L_{p,A,S,n}$ at each source to receiver distance r_n, where n denotes the measurement position, the regression line and $L_{p,S,4m}$ should also be included in the graph. A second graph of the STI versus measurement position, r_d, r_p and regression line should also be included.

The ISO 3382-3 does not provide recommended values, but two examples are included in the appendix, one example showing poor and one showing good acoustical conditions.

NS 8175 however provides recommended values for classed A-D, where class A is excellent acoustical conditions and D is poor. NS 8175 is self-contradicting, since class A background noise is less than 28dB(A), while class A r_d is less than $5m$. The STI is highly dependent on the background noise level, a low BGN results in a high STI which in turn results in a long r_d. In Norway most building regulations require Class C or lower for the background noise level.

Chapter 4

Method

4.1 The office layout

The office is the COWI office in Oslo, Karvesvingen 2 at the 4th floor. Measurements were done in two Zones of the office, shown in figure 4.1. These two Zones were chosen since they had different geometry and the workstations (desks) had different spacing. The Zones have small connecting corridors to the other parts of the office, these corridors were modeled as fictive walls. This made it possible to look at each of the two Zones as separate rooms. For each Zone, measurements were done along one line with the source placed in the outer workstation (desk) at opposite sides of the lines. 4 to 5 measurement positions were chosen across each line.

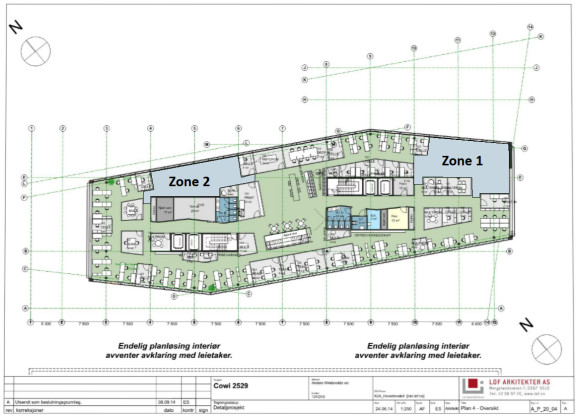

Figure 4.1: Layout of the office, showing Zone 1 and Zone 2

Figure 4.2 - 4.3 shows the two Zones and ML1 for each of the Zones. ML 1 and 2 have the source at the opposite sides of the lines, and the measurement lines are measured in opposite directions. For ML 2 the source position is S_2 and it is in receiver position

4, R_4. According to ISO 3382 [2], the speaker and microphone should be placed more than $0,5m$ from tables, and more than $2,0m$ from walls and other reflecting surfaces. The source and receiver were both place at height $1,2m$ above the floor. The receivers were placed close to the center of each desk. (Standing workstations are not covered by this part of ISO 3382-3.).

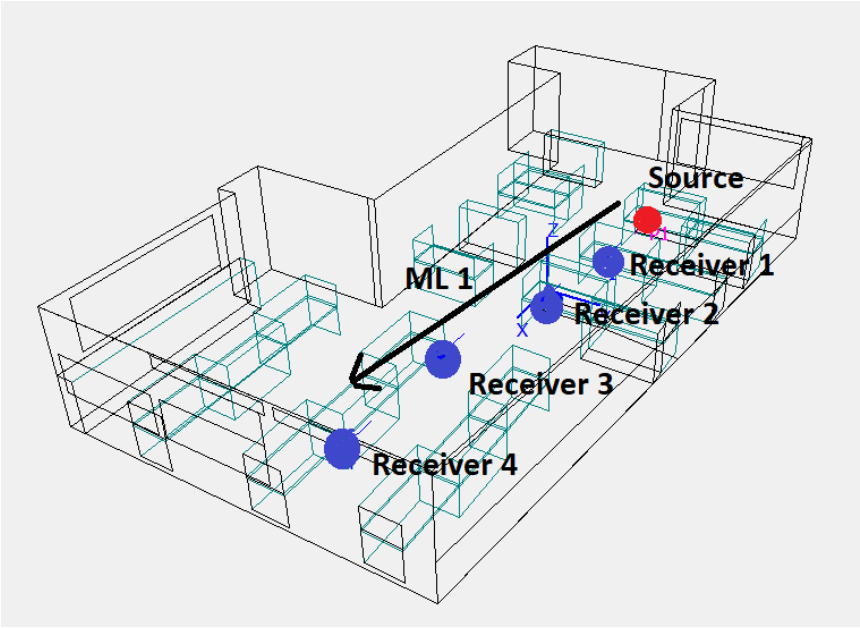

Figure 4.2: Zone 1, with furnishing

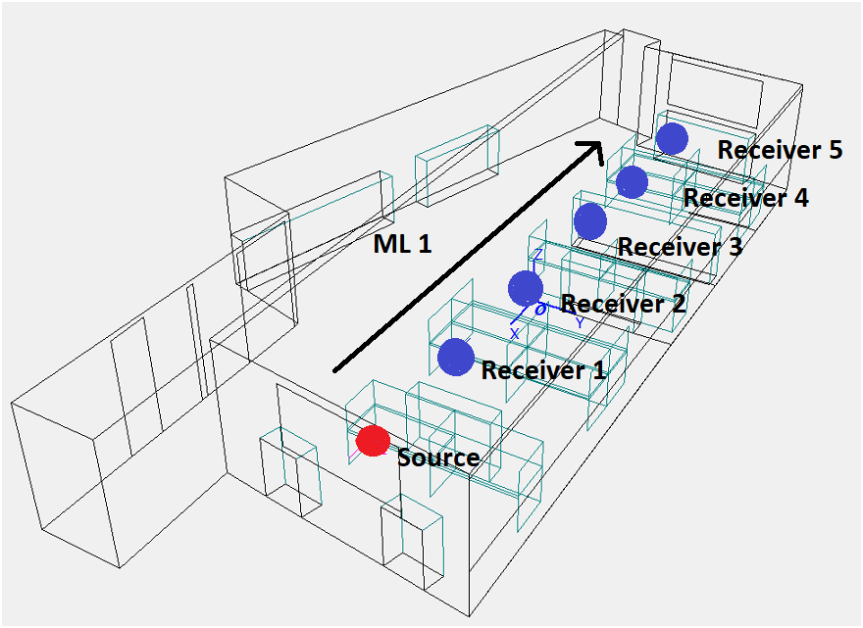

Figure 4.3: Zone 2, with furnishing

Figures 4.4 - 4.5 show the first position in ML1 for the two Zones.

Figure 4.4: Picture from Zone 1

Figure 4.5: Picture from Zone 2.

4.2 Measurements

The measurements of the impulse responses, IR, were performed at the COWI office from 18:00-00:30 O'clock on the 22nd of April 2017. The measurements were done in furnished rooms, with no people present, except the one needed to do the measurements. Systems for heating, ventilation and conditioning, and other sources of sound were not driven with the same effect as during working hours. ISO 3382-3 [2] recommends that they should be, but the ventilation was automated and could not be changed easily. Additional measurements of the daytime background noise level were done at 17:00-18:00 oclock the 25 of April 2017. This was the best representation of the background noise level during working hours possible to obtain. For these measurements, systems for heating, ventilation and conditioning, and other sources of sound were were driven with the same effect as during working hours, as recommended by ISO 3382-3 [2]. Figure 4.6, shows the measurement system used.

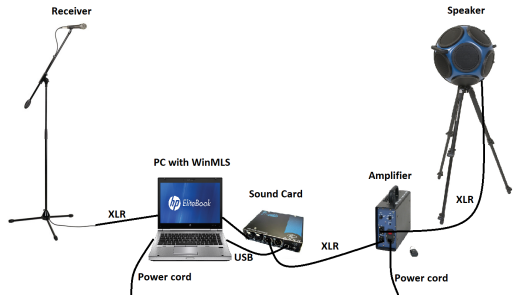

Figure 4.6: Measurement system

The sound card was connected to a PC with WinMLS via the USB 2.0 port. For the sound card, and internal loop back from input B to output B was set in the sound card settings. The loop back makes it possible to know the exact time the speaker starts to play. The input port A was connected to the microphone and the output A was connected to the amplifier that in-turn was connected to a power socket and the speaker.

A measurement of the system delay was done according to ”4.3 measurement 1” in the WinMLS User Guide [22]. The sound card had a 40 sample delay, this delay was adjusted for in WinMLS, such that the impulse response started at the same time as the signal was played from the speaker. The system delay with the USB 3.0 port gave an unwanted effect, and was therefore not used. The unwanted effect was that when sending a single pulse, three consecutive pulses were measured when using the USB 3.0 port.

The background noise level was measured in Zone 1 and 2. The measurement setups is the same as above, only now the speaker and amplifier are removed. The system was calibrated using a calibrator with 113.8dB at 1kHz. A measurement of the level with the calibrator attached was taken to be able to calculate the level difference between WinMLS and Matlab. As mentioned, two sets of measurements of the background noise level were done, one at night and one at day time. For the night time background noise level measurements, $10s$ impulse responses were measured in 9 random positions at different heights in Zone 1 and Zone 2. Only the author was present.

The day time measurements were done at each of the positions along the measurement lines, ML, and $20s$ impulse responses were measured to make the measurements more robust against fluctuating noise. For measurements in Zone 1 the author and two other people were present, but they were quiet during the measurements. In Zone 2 only the author was present, but other people were in the office outside Zone 2.

The impulse responses in Zone 1 were measured. The measurement setup shown in Figure 4.6 was used. For this measurement setup, the impulse responses along the two lines were measured. The receiver was placed at the center of the desks. The sound card setup was uploaded to WinMLS and D-audio was chosen. For the D-audio volume mixer, the ”loopback right” and ”phantom left” were turned on. The measurement setup ”Time and frequency response”, under ”General” was chosen. The measurement setting were 2.2s ”maximum expected decay”, and $20s$ ”total duration of measurement”. Signal type was ”sinus-sweep”, and the range was set from $40Hz - MaxHz$. The calibration was double checked. Measurements were done according to ISO 3382-3, only the author was

present. An omni-directional whole sphere speaker was used, the speaker was adjusted such that the SNR was more than $45dB$ at the furthest position in Zone 2. The measurements in Zone 1 were done along ML 1 and 2, as shown in Figures 4.2. Keep in mind that the sine sweep method attenuates the background noise. The method gives a better SNR than the measured level minus the background noise level. The setup was moved to Zone 2, and measurement were done along the measurement line shown in figure 4.3.

For both Zones, part of the ISO 3382-3 was not fulfilled. As mentioned earlier, the standard states that the source and receiver should be more than $2m$ away from other reflecting surfaces. This was not possible to fulfill due to the length of the room and the workstation layout. For Zone 1 R_4 was $0.986m$ away from the back wall. For Zone 2 the source position and R_5 were $1.24m$ and $1.30m$ away from the back walls, respectively.

A reference measurement at $1m$ source to receiver distance was taken. The measurement was done in the most open place in the office. The source and receiver were $1.2m$ and $1.5m$ from the ceiling. The distance between the receiver and the back wall was $2m$.

All the measured impulse responses were stored as ".wmb" files, and were imported to Matlab using WinMLS "loadimp" function for post processing. The reverberation time was estimated in WinMLS, the other parameters were all estimated in Matlab.

4.2.1 Equipment

List of equipment:

- Calibrator: NorSonic Sound Calibrator type 1251. ID: Nor1251-29901
- Measurement PC: hp Elitebook 2570p with WinMLS
- Microphone BSW4000, COWI nr 4502562 with pre-amplifier
- Speaker: Whole sphere Nor 276, serial no. 2765795.
- Amplifier: NOR 280, serial no. 2804152.
- Soundcard: D-audio, AXYS, serial no. 009900092
- Miscellaneous stands and XLR-cables

Figure 4.7: Nor276 whole sphere speaker

The sound source used was a whole sphere speaker type Nor276, see Figure 4.7. ISO 3382-3 [2], specifies that a deterministic signal with a pink spectrum should be used, which is fulfilled by a log sine-sweep. The source has to meet the demands of ISO 3382-1 [1], which require the source to be omni-directional with maximum acceptable deviation when averaged over "glinding" 30° arcs in a free sound field. Table 4.1 shows the maximum values per octave band from ISO 3382-1 [1].

Table 4.1: Maximum deviation of directivity in dB for excitation with octave bands of pink noise and measured in free field, ISO 3382-1 [1]

Frequency [Hz]	125	250	500	1000	2000	4000
Maximum deviation [dB]	$\pm$ 1	$\pm$ 1	$\pm$ 1	$\pm$ 3	$\pm$ 5	$\pm$ 6

Figure 4.8 shows the maximum and minimum directivity of the speaker according to the specification of ISO 3382-1 [1] with the tolerance limits from the table above.

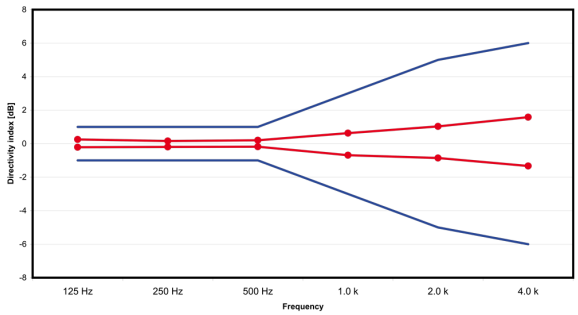

Figure 4.8: Nor276 whole sphere speaker directivity (red line) versus the ISO 3382-1 max deviation of direktivity (blue line), with reference to Norsonic's website [23]

Figure 4.9 shows the sound power of the speaker. The measurements have been done

in a horizontal plane, and a sinus signal of 1/3-octaves 100Hz, 315Hz, 1kHz and 3.15kHz are plotted, reference made to Norsonic's website[23].

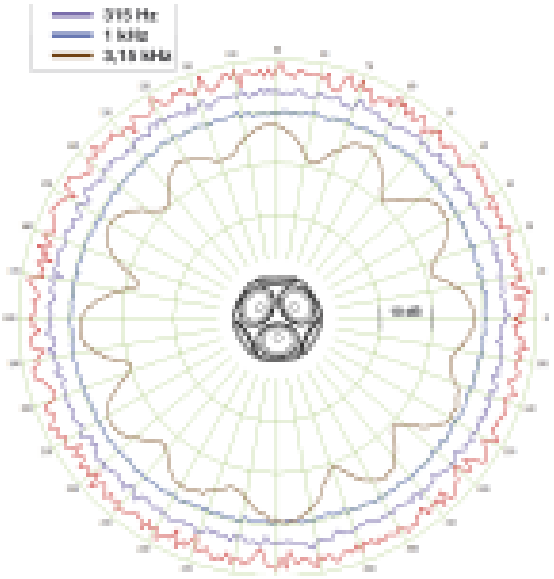

Figure 4.9: Nor276 whole sphere speaker sound power in different directions, see Norsonic's website [23]

The frequency response of the source is shown in Figure 4.10. The frequency response is estimated in 1/1 octave bands and 1/3 octave bands.

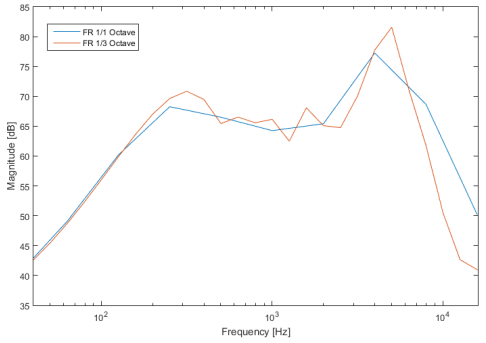

Figure 4.10: Frequency response of the source in 1/1 and 1/3 octave band values.

The receive is omni-directional and fulfills the demands of a class 1 receiver, from NEK EN 61672-1 [4].

4.3 Simulation

Simulations was done using Odeon 14 Combined, [9]. Models of the two Zones were made in Sketchup and imported to Odeon using Odeon's plugin, SU2Odeon. For each of the two Zones a simple model was made and the connecting corridors were modeled as fictional surfaces. Absorption and scattering coefficients were chosen, such that the measured and simulated RT were close. The simulation measurements were done as close to the same positions as for the real measurements.

The measured sound pressure level and source receiver distance was stored along with the impulse response for each of the measurement positions. The impulse responses were stored as ".wav" files. As the ".wav" files are normalized to $+/-1$, the sound pressure level was used to estimate a scaling factor for each measurements. The impulse responses from Odeon were stored and used for estimating STI and the other ISO 3382-3 parameters with the same functions as for the measurements. This was done to reduce uncertainties due to processing. The reverberation time was estimated in Odeon. Note that the impulse responses attained from Odeon are noise free. Under the calculation parameters setup, precision was selected. Figure 4.11 shows the calculation parameters used.

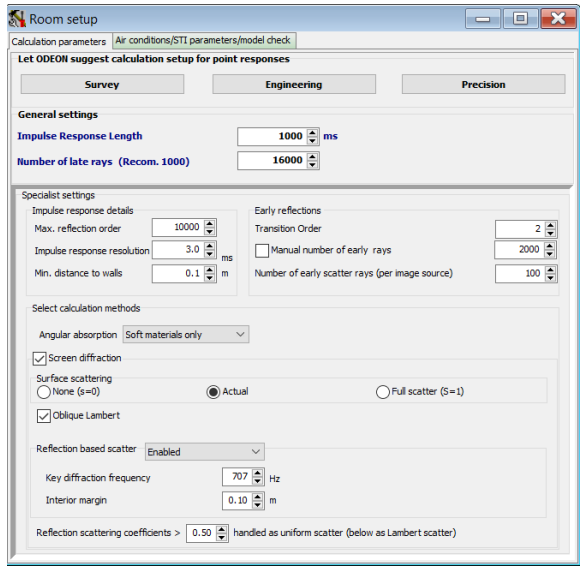

Figure 4.11: Calcuation paramters in Odeon.

The stored ".wav" files were neutral impulse responses, to obtain these from Odeon some steps are required. First under "Tools/Create Filtered HRTF" option, the file "unity.ascii_hrtf" is to be selected. Second, under "auralization setup", the "unity" file has to be chosen and "headphones" need to be turned off.

A single point response "job" was made for each combination of source and receiver positions, and run individually. The "play single point impulse response" button was pressed, and then the IR was stored. The neutral impulse responses produced are short,

they contain about half of the sampling frequency, FS, in samples which corresponds to an IR length of $0.5s$. The length of each IR is different.

In Odeon one can calculate single point, multipoint or grid responses. The single point responses were used for making the IR's and the multipoint responses were made for estimating RT and all the ISO 3382-3 parameters in Odeon. The grid response is a great tool for assessing if there are areas that have unreasonably high RT in one or more octavebands.

For the simulations, the "Omni ISO3382" point source was used, giving a SPL at 1m according to ISO 3382-3. The receivers were point receivers.

4.3.1 Materials

The absorption and scattering coefficients of the materials in offices had to be determined. The reverberation time was known, so the reverberation time for the simulation could be adjusted to fit to the measured RT. The ceiling and floor were know and data sheets are given in Appendix D. Odeon has a large library of measured absorption coefficients for different materials, this was also used as a guide line for probable values. Probable values for each of the materials were chosen and adjusted such that the simulated RT fit the measured RT.

The screens were modeled all the down to the floor, this was to compensate for not modeling chair, and to reduce complexity of the model. From Figure **??** we see how the actual screen were.

From multiple simulations, two simulation models were chosen to be looked at further. Two simulation models were made and each model contained two Zones. The main difference between the simulation models is that simulation model 1 had the same absorption and scattering coefficients in both Zones, while simulation model 2 had some differences between the two Zones. Another difference between the two simulation models is that for model 2, the desk has a thickness of 5cm, and the top of the desk is given a slightly higher scattering. The top of the cabinets are also given a higher scattering. For simulation model 1, the thickness of the desk is zero and the entire desk and cabinets have the same scattering. Table 4.2 lists the absorption and scattering coefficients for the materials in simulation model 1. These coefficients were chosen after multiple trials, that started with values from data sheets in Appendix D and the suggested values from the Odeon library.

Two types of suspended ceiling were used in the office, Tropic and Krios. The suspended ceilings have a thickness of $40mm$ and $15mm$, respectively. The absorption coefficient for Tropic given in Appendix D.1 and for Krios in Appendic D.2. Appendix D.3 shows were each of them was used, "Standard himling" is Tropic, and "Lyd himling" is Krios. In Zone 2, both types of suspended ceiling were used. The lower hanging part was Krios, while the higher part was Tropic. Zone 1 only had the Krios ceiling. The flooring is called Epoca structure and has an acoustic absorption of $0.15aW$, from a data sheet Appendix D.4. The material "needled felt" from the Odeon library was chosen to represent it. The walls have been modeled as 13mm plaster with 100mm mineral wool, from Odeons library. Rock Sonar 40dB is the name of 40mm thick plates that were hanged on the walls in opposite sides of the office. The exterior and interior windows were modeled from Odeons library and were called "Glass ordinary window glass (Harris 1991)" and "single pane of glass (ref Multiconsult, Norway)", respectively. The screens were called 8 Duba

Table 4.2: Simulation model 1, Zone 1 and 2, material/surface absorption and scattering coefficients, s denotes the scattering coefficient.

	Absorption coefficient							
Material	**125**	**250**	**500**	**1000**	**2000**	**4000**	**8000**	**s**
Tropic	0.45	0.95	1	1	1	1	1	0.11
Krios	0.55	0.90	1	1	1	1	1	0.11
Epoca structure	0.01	0.05	0.10	0.20	0.30	0.40	0.40	0.05
Wall	0.28	0.14	0.12	0.09	0.06	0.02	0.01	0.04
Rock Sonar 40dB	0.15	0.55	1	1	1	1	1	0.05
Exterior window	0.35	0.25	0.18	0.12	0.07	0.04	0.04	0.15
Interior window	0.18	0.06	0.04	0.03	0.02	0.01	0.01	0.06
Screen	0.10	0.26	0.42	0.63	0.80	0.93	0.90	0.04
Desk	0.10	0.07	0.05	0.06	0.06	0.06	0.06	0.03
Cabinets	0.1	0.09	0.09	0.09	0.04	0.02	0.01	0.05
Fictive Zone 1	0.70	0.70	0.70	0.70	0.70	0.70	0.70	0.3
Fictive Zone 2	0.90	0.90	0.90	0.90	0.90	0.90	0.70	0.3

Desk screen, with Cara Camira EJ033 textile covering, but coefficients were unknown. The screens were modeled after another similar screen, i.e. model 4Q from Hovem furniture industry, and the coefficients were altered. The model 4Q screen is nr 7 in Appendix D.5. There is large uncertainty related to the screen modeling. The desks were given the absorption coefficients for a ”Floating wooden floor”, in the Odeon library. The Cabinets were given similar absorption as the desks. The fictional surface was given a high absorption as it is likely that little sound would reflect back. The fictional surfaces for the two Zones were given different values as the fictional surfaces in Zone 1 seemed more likely to have returning sound than those in Zone 2. This was due to the geometries of the spaces and materials behind the fictional surfaces.

The scattering coefficients in both Zones were chosen based on likely values. Since the model is flat, parts such as windows that were not flat in reality were given a higher scattering coefficient rather than making a detailed model.

Tables 4.3 - 4.4 show the scattering and absorption coefficient for simulation model 2, Zone 1 and Zone 2.

Table 4.3: Simulation model 2, Zone 1, material/surface absorption and scattering coefficients, s denotes the scattering coefficient.

	Absorption coefficient							
Material	**125**	**250**	**500**	**1000**	**2000**	**4000**	**8000**	**s**
Krios	0.55	0.70	0.80	0.90	1	1	1	0.11
Epoca structure	0.01	0.02	0.05	0.15	0.3	0.4	0.4	0.05
Wall	0.28	0.14	0.12	0.09	0.06	0.02	0.01	0.04
Rock Sonar 40dB	0.15	0.55	1	1	1	1	1	0.05
Exterior window	0.35	0.25	0.18	0.12	0.07	0.04	0.04	0.10
Interior window	0.18	0.06	0.04	0.03	0.02	0.01	0.01	0.06
Screen	0.10	0.26	0.42	0.63	0.80	0.90	0.90	0.04
Desk	0.1	0.07	0.05	0.06	0.06	0.06	0.06	0.03
Desk top	0.1	0.07	0.05	0.06	0.06	0.06	0.06	0.04
Cabinets	0.10	0.09	0.09	0.09	0.04	0.02	0.01	0.05
Cabinets Top	0.10	0.09	0.09	0.09	0.04	0.02	0.01	0.15
Fictive Zone 1	0.70	0.70	0.70	0.70	0.70	0.70	0.70	0.3

Table 4.4: Simulation model 2, Zone 2, material/surface absorption and scattering coefficients, s denotes the scattering coefficient.

	Absorption coefficient							
Material	**125**	**250**	**500**	**1000**	**2000**	**4000**	**8000**	**s**
Tropic	0.45	0.90	0.1	0.90	1	1	1	0.11
Krios	0.55	1	1	0.95	1	1	1	0.11
Epoca structure	0.01	0.05	0.08	0.16	0.3	0.4	0.4	0.05
Wall	0.30	0.16	0.14	0.10	0.05	0.02	0.01	0.04
Rock Sonar 40dB	0.15	0.55	1	1	1	1	1	0.05
Exterior window	0.35	0.25	0.18	0.12	0.05	0.02	0.01	0.15
Interior window	0.18	0.06	0.04	0.03	0.02	0.01	0.01	0.06
Screen	0.10	0.29	0.45	0.66	0.83	0.92	0.92	0.04
Desk	0.10	0.07	0.05	0.06	0.06	0.04	0.04	0.03
Desk top	0.10	0.07	0.05	0.06	0.06	0.04	0.04	0.04
Cabinets	0.10	0.09	0.09	0.09	0.04	0.02	0.01	0.05
Cabinets Top	0.10	0.09	0.09	0.09	0.04	0.02	0.01	0.09
Fictive Zone 1	0.85	0.80	0.80	0.80	0.80	0.70	0.70	0.3

The materials are the same as for model 1, but with slightly different values such that the simulated RT better fits the measured RT. As mentioned earlier, the scattering on the top of the desks and cabinets was higher due to more objects being on top of them. The scattering on top of the cabinet had a large impact on the RT. The desks had about the same amount of clutter in both Zones. The cabinets had more clutter on top of them in Zone 2 than in Zone 1, but too make the RT more similar to the measured values, the scattering had to be higher for this material in Zone 1.

4.3.2 STI estimation

It is desirable to estimate the STI in the same way for measurement and simulations. Odeon and WinMLS both estimate STI according to IEC 60268-16, 2003 [4]. The implementation might not be the same in Odeon and WinMLS, so a function to estimate the STI was implemented in Matlab. This ensures that all results are processed in exactly the same way. The Matlab function estimates STI according to IEC 60268-16 [5], and given in Appendix A.1. The function has three inputs, an impulse response, BGN and sound pressure level of speech at $1m$. The function first adjusts the level of the impulse response, then octave band filters and find the equivalent level of each octave band. Then it finds the SNR between the BGN input and the adjusted impulse response, and uses this to estimate the STI using Jacob Donleys STI function [13].

The ISO 3382-3 standard [2] specifies that for an OMNI source, the sound pressure level of speech at $1m$, $L_{p,S,1m}$, is $49.5db$, $54.3dB$, $58.0dB$, $52.0dB$, $44.8dB$, $38.8dB$ and $33.5dB$ for the $125Hz - 8kHz$ octave bands, giving an A-weighted sum of $57.4dBA$. ISO 3382-3 refers to ANSI S 3.5-1997 [3].

It is hard to verify the STI function. A simple test of the STI in ideal conditions gives a rough verification. Odeon was used to measure make a noise free measurement at $1m$, in free field. This measurement should given an STI of 1. The SPL at 1m was -11 in all bands, and 100dB BGN was added to the IR, not the STI should be 0. Using the function on the previous IR's gave STI values of respectively 0.998 and 0.0217. This shows that the function is in the right ball park, but does not verify the function.

A few tests were done to see the difference in STI, when estimated using the Matlab function from the STI estimated using Odeon and WinMLS.

Table 4.5 shows the STI estimated using WinMLS versus the matlab function. The results are when using a background noise level of $21.4dB$, $24.3dB$, $22.7dB$, $18.5dB$, $18.1dB$, $18.0dB$ and $16.9dB$ and $L_{p,S,1m}$ of $67dB$, $67dB$, $65dB$, $58dB$, $52dB$, $48dB$ and $40dB$ for the $125 - 8kHz$ octave bands on measurement in Zone 1 ML1.

Table 4.5: STI in WinMLS versus Matlab

	Position	**1**	**2**	**3**	**4**
STI	**WinMLS**	0.84	0.75	0.69	0.68
	Matlab	0.85	0.78	0.72	0.72

Table 4.6 shows the STI estimated using Odeon versus the Matlab function. This is when using back ground noise level of $37.5dB$, $32.9dB$, $25.9dB$, $18.5dB$, $16.9dB$,

$17.0dB$ and $18.0dN$ for the $125 - 8kHz$ octave bands and $L_{p,S,1m}$ as for OMNI source described above, on simulations model 1 in Zone 1 ML1.

Table 4.6: STI in Odeon versus Matlab

	Position	**1**	**2**	**3**	**4**
STI	**Odeon**	0.75	0.57	0.55	0.55
	Matlab	0.75	0.57	0.57	0.56

The Matlab STI function seems to slightly overestimate the STI, compared to WinMLS and Odeon.

Chapter 5

Results

This Chapter presents results of the background noise level and the reverberation time. The background noise level is an input for the STI estimation. The simulated RT depends on the absorption and scattering coefficient chosen for the Odeon model. Subsequently, the A-weighted SPL based parameters and the STI based parameters are assessed. As mentioned earlier, these parameters have been estimated using the same Matlab functions. Finally, the correlation between the parameters are presented. Some discussion of the results is also given here, rather than having a too long discussion in Chapter 6.

5.1 Background noise level

The background noise levels were measured as stated in Chapter 4. Odeon makes noise free simulations, so the impulse responses attained from Odeon are noise free.

The background noise levels during night, at day and for noise criterion 25, NC 25, are shown in Table 5.1. The criterion was found in settings for STI estimation in Odeon. The levels are given in $1/1$-octave band values from $125Hz - 8kHz$. The results called "BGN night" show the background noise level in the office when the measurements were done at night. The "BGN day" shows the background noise level measured in working conditions during day time. NC 25, has been chosen to evaluate the effect of increased background noise level on the STI.

Table 5.1: 1/1 octave band background noise level, and sum $L_{p,A,B}[dBA]$ for Zone 1-2.

Freq [Hz]	125	250	500	1000	2000	4000	8000	Total
Zone 1								
BGN night [dB]	27.16	19.94	15.91	14.46	14.67	16.00	17.57	23.14 [dB(A)]
BGN day [dB]	37.52	32.85	25.93	18.52	16.89	16.95	17.97	29.24 [dB(A)]
Zone 2								
BGN night [dB]	31.73	21.54	17.62	13.89	14.50	15.78	17.75	23.80 [dB(A)]
BGN day [dB]	45.63	29.60	24.96	19.75	17.15	17.11	18.25	31.62 [dB(A)]
Both								
NC 25	44	37	31	27	24	22	21	34.83 [dB(A)]

The ISO 3382-3 [2] specifies that the BGN shall be measured in each of the measurement positions, and that the average A-weighted BGN shall be used for estimating STI. Only the BGN day was done at the measurement position, the BFN night was done at 9 random positions in the room.

BGN day for both Zones is less than $33dB(A)$ and more than $28dB(A)$, thus it is in class C og NS 8175 [6]. Class C is usually a requirement for office spaces. The NC 25 has total A-weighted BGN of $34.8dB(A)$ which puts it in class D.

5.2 Reverberation time

The reverberation time was estimated using WinMLS for the measurements, and Odeon for the simulations. The reverberation time used through out this thesis is T_{30}. The mean RT measured from all microphone positions of ML1 in Zone 1 and 2 are given in Table 5.2 below. This means the RT for Zone 1 was measured from the four receiver positions shown in Figure 4.2, and the RT in Zone 2 was measured from the five receiver positions shown in Figure 4.3. The RT has been measured and simulated in the same positions, and the RT at each position is given in Appendix C.

Fitting the simulated RT to the measured RT is not easy. The octave bands from $2kHz$ and above are highly dependent on the air absorption, and very tricky to adjust. More focus was put on the RT below $2kHz$, since the air absorption becomes the dominant absorption above this frequency. A higher scattering, will result in a lower RT for the high frequencies, due to the air absorption.

The number of rays used for the estimation has a large impact on the RT, using less than 16000 rays give large variations in RT.

Table 5.2: Reverberation time, $T30$ Zone 1 and 2

Freq [Hz]	125	250	500	1000	2000	4000	8000
Measured							
Zone1 [s]	0.41	0.35	0.31	0.32	0.38	0.39	0.38
std	0.04	0.02	0.02	0.03	0.04	0.06	0.05
Zone 2 [s]	0.38	0.31	0.28	0.30	0.36	0.37	0.37
std	0.03	0.02	0.03	0.02	0.04	0.03	0.02
Simulation model 1							
Zone 1 [s]	0.4	0.34	0.3	0.31	0.35	0.35	0.28
std	0.01	0.01	0.01	0.01	0.03	0.03	0.02
Zone 2 [s]	0.39	0.35	0.36	0.38	0.4	0.41	0.35
std	0.0	0.02	0.04	0.03	0.02	0.02	0.02
Simulation model 2							
Zone 1 [s]	0.4	0.34	0.31	0.31	0.32	0.37	0.29
std	0.01	0	0	0.01	0.01	0.08	0.01
Zone 2 [s]	0.38	0.29	0.28	0.3	0.31	0.34	0.28
std	0.0	0.02	0.04	0.03	0.02	0.02	0.02

Figures 5.1 - 5.2 show the values for the measured RT with the standard deviation and simulated RT's from Table 5.2 for Zone 1 and 2, respectively. The $4kHz$ simulation model 2 and Zone 1 has a large standard deviation. From RT table in Appendix C.3 we see that there are large variations for simulation model 2 Zone 1. For measurement position 4 the RT is $0.49s$ and for position 2 it is $0.31s$.

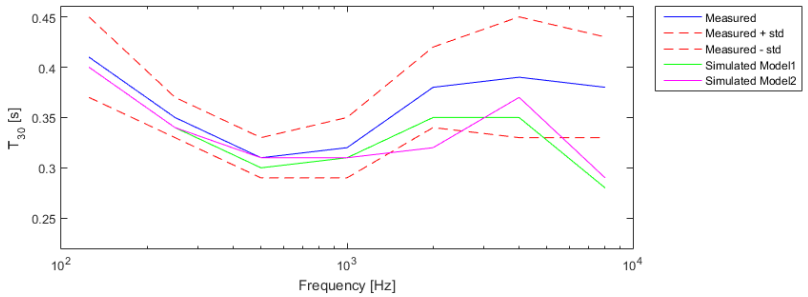

Figure 5.1: RT in Zone 1, measured, measured $\pm$ standard deviation and simulated using simulation model 1 and 2.

From Figure5.1 it is difficult to claim which model fits the measured data best over the entire frequency range. Simulation model 2 fits best at 500Hz and 4kHz, and simulation model 2 fits best at 2kHz. Simulation model 1 has a curve that follows the measured data a little bit better than simulation model 2.

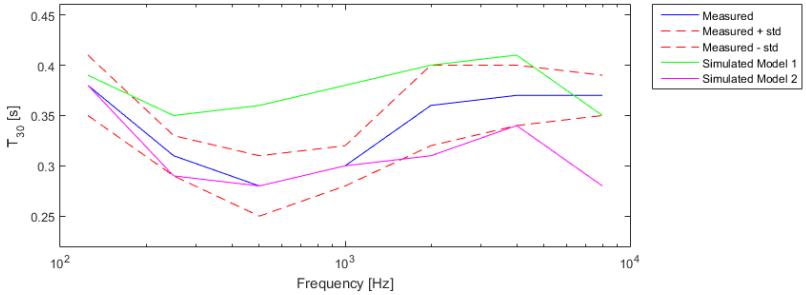

Figure 5.2: RT in Zone 2, measured, measured $\pm$ standard deviation, and simulated values using simulation model 1 and 2.

From Figure 5.2 simulation model 2 seems to fit better than simulation model 1. Simulation model 1 overestimates the RT, while model 2 underestimates it. The measure reverberation times in the two Zones has a dip from $250Hz - 1kHz$, this is unexpected as the room has a lot of high frequency absorption. An explanation might be that there is a coupled room effect. Another explanation might be that there is a flutter effect for the high frequencies. The ceiling and floor is highly absorbent for the high frequencies, but the walls and windows are less absorbent, especially for high frequencies, as shown in Chapter 4.3.1. The air is also highly absorbent for the high frequencies, so even with flutter one would expect a faster decay above $2kHz$.

5.3 A-weighted SPL based parameters

Tables 5.3-5.4 show the measured and simulated values for the A-weighted SPL of speech at measurement position n, $L_{p,A,S,n}$, and the S-R distance at measurement position n, r_n, for Zone 1 and 2, ML1 and 2.

Table 5.3: Zone 1, $L_{p,A,S,n}$ and r_n

Model	**Position nr.**	**1**	**2**	**3**	**4**
ML 1					
Measured	**r_n [m]**	1.96	4.84	6.71	9.89
	$L_{p,A,S,n}[dB]$	52.6	45.8	44.3	41.9
Simulation model 1	**r_n [m]**	2.10	4.28	6.91	9.88
	$L_{p,A,S,n}[dB]$	48.8	43.0	42.1	40.8
Simulation model 2	**r_n [m]**	2.10	4.28	6.91	9.88
	$L_{p,A,S,n}[dB]$	48.7	43.0	44.4	41.3
ML 2					
Measured	**r_n [m]**	3.29	5.24	8.12	10.14
	$L_{p,A,S,n}[dB]$	52.9	50.1	45.2	41.6
Simulation model 1	**r_n [m]**	3.00	5.60	7.68	9.88
	$L_{p,A,S,n}[dB]$	53.0	48.4	41.6	40.5
Simulation model 2	**r_n [m]**	3.00	5.60	7.68	9.88
	$L_{p,A,S,n}[dB]$	53.2	49.6	41.9	40.6

The measurement positions 1-4 along ML1 are the ones shown as receiver position 1-4. For ML2 the source is placed on the opposite side of the measurement line, and measurement position 1-4 start at receiver position 3 and end at the source position for ML1. The same is the case for Zone 2 although for Zone 2 there are 5 measurement position and ML2 starts at receiver position 4.

From Table 5.3 we see that the measured and simulated source to receiver distance r_n are fairly similar. For ML1 the measured $L_{p,A,S,n}$ is larger than the simulated for all positions, and the deviation get smaller the further away we go.

The $L_{p,A,S,n}$ for simulation model 2 ML1 is lower in measurement position 2 than in measurement position 3. From Figure 4.2 it looks like measurement position 3 is more exposed to sound, while measurement position 2 is more hidden. This is not the case for simulation model 1, it might be due to scattering choices.

For ML 2, the measured and simulated $L_{p,A,S,n}$ are close, although measurement position 3 is much more damped for the simulation than for the measurements.

Table 5.4: Zone 2, $L_{p,A,S,n}$ and r_n

Model	**Position nr.**	**1**	**2**	**3**	**4**	**5**
ML 1						
Measured	**r_n [m]**	2.58	4.82	7.58	9.80	12.38
	$L_{p,A,S,n}[dB]$	53.4	46.8	42.9	40.5	35.8
Simulation model 1	**r_n [m]**	2.60	5.32	8.42	10.35	13.17
	$L_{p,A,S,n}[dB]$	47.7	42.3	38.8	38.0	37.2
Simulation model 2	**r_n [m]**	2.60	5.15	8.1	10.35	12.9
	$L_{p,A,S,n}[dB]$	44.2	39.6	39.4	38.5	36.7
ML 2						
Measured	**r_n [m]**	2.36	4.89	7.54	8.69	12.39
	$L_{p,A,S,n}[dB]$	51.5	49.0	41.1	37.6	35.6
Simulation model 1	**r_n [m]**	2.87	4.80	7.91	10.62	13.22
	$L_{p,A,S,n}[dB]$	45.9	42.9	41.1	37.9	37.9
Simulation model 2	**r_n [m]**	2.55	4.80	7.75	10.3	12.9
	$L_{p,A,S,n}[dB]$	44.6	43.6	41.7	37.9	37.7

From Table 5.4 we see that the measured and simulated source to receiver distance r_n are fairly similar. For ML1 the measured $L_{p,A,S,n}$ is higher than the simulated, the deviation get smaller the further away we go. Simulation model 1 is much higher for measurement positions 1 and 2.

For ML2 the measured $L_{p,A,S,n}$ is about $7dB$, $6dB$ and $2dB$ higher than the simulated for measurement positions 1, 2 and 5, respectively. For measurement position 3 and 4 the measured and simulated values are quite similar. The simulated $L_{p,A,S,n}$ is very similar for both simulation models.

Figures 5.3-5.5 show $L_{p,A,S,n}$ versus r_n from Tables 5.3-5.4. The figures are plotted according to ISO 3382-3 [2]. $L_{p,A,B,n}$ is from "BGN day", at each of the measurement positions, n. $L_{p,A,S,n}$ is independent of the BGN.

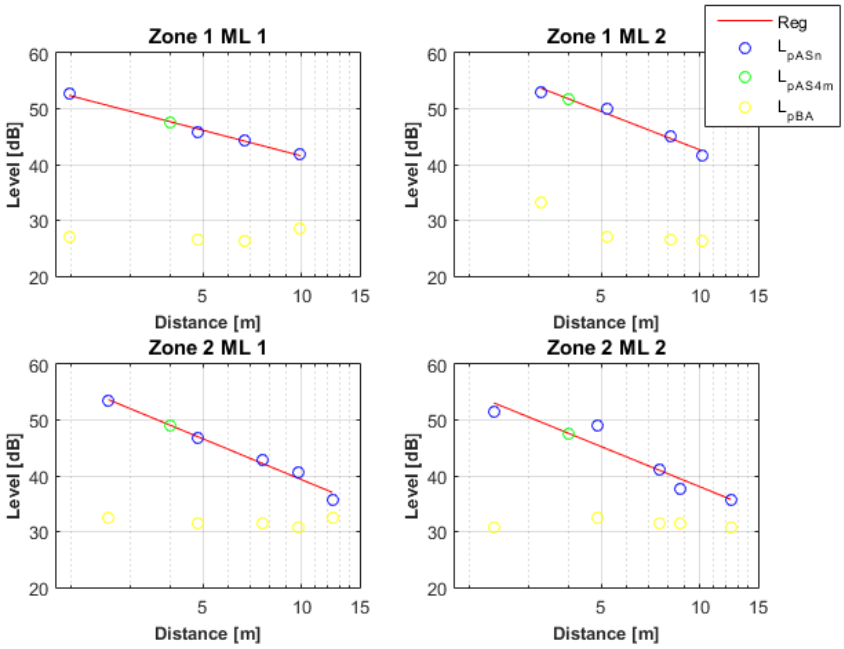

Figure 5.3: Measured, A-weighted speech level versus S-R distance.

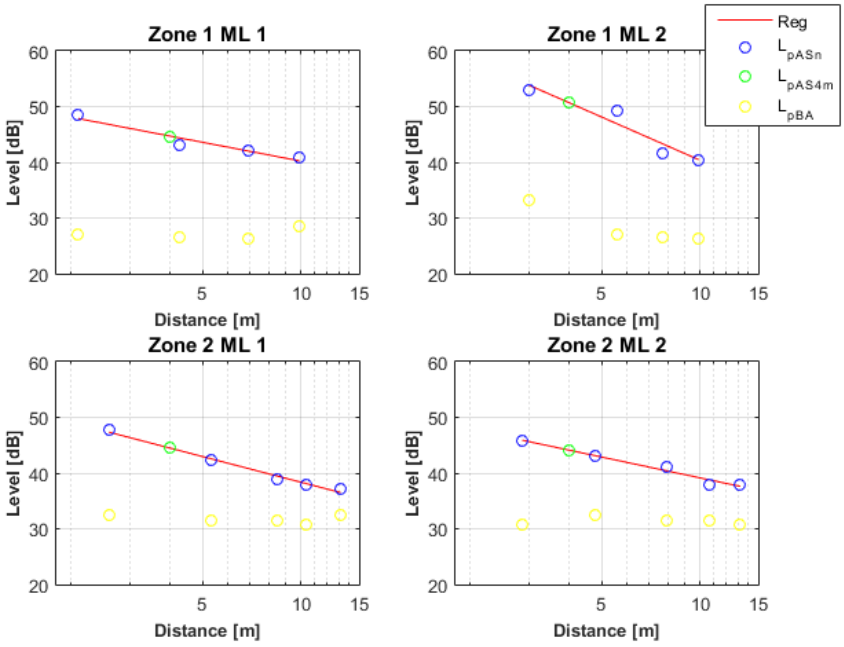

Figure 5.4: Simulation model 1, A-weighted speech level versus S-R distance.

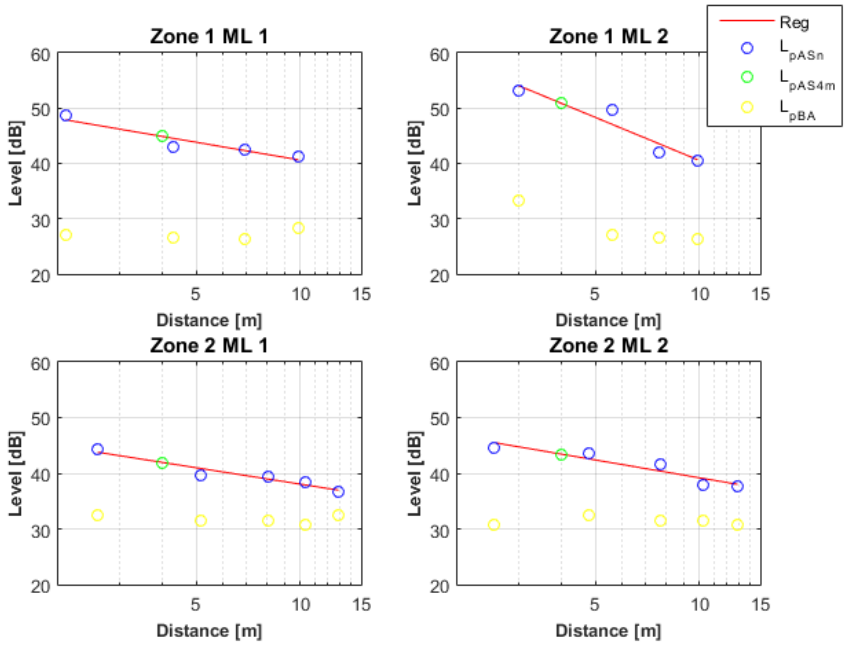

Figure 5.5: Simulation model 2, A-weighted speech level vs S-R distance.

The regression line shows the distance attenuation. We can also see how far over the background noise level we are. Further we can see if there are some irregularities for the $L_{p,A,S,n}$. $L_{p,A,S,n}$ measured in Zone 2 ML2 is about $4dB$ over the regression line at measurement position 2, this is not the case for the simulation models.

The A-weighted SPL based parameters ($D_{2,s}$, $L_{p,A,S,4m}$, $L_{p,A,B}$) are given in Table 5.5. $D_{2,s}$ is estimated according to Equation 3.4, $L_{p,A,B}$ is the mean of "BGN day", while $L_{p,A,S,4m}$ was read from Figures 5.3 - 5.5.

Table 5.5: Measured and simulated A-weighted SPL based parameters, Zone 1 and 2.

Zone & ML	$D_{2,s}[dB]$	$L_{p,A,4m}[dBA]$	$L_{p,A,B}[dBA]$ "BGN day"
Measured			
Zone1 & ML1	4.6	47.6	29.2
Zone1 & ML2	6.9	51.7	29.2
Zone2 & ML1	7.4	49.0	31.6
Zone2 & ML2	7.2	47.6	31.6
Simulated 1			
Zone1 & ML1	3.4	44.7	29.2
Zone1 & ML2	7.8	50.7	29.2
Zone2 & ML1	4.6	44.5	31.6
Zone2 & ML2	3.8	44.1	31.6
Simulated 2			
Zone1 & ML1	3.2	44.8	29.2
Zone1 & ML2	7.8	50.9	29.2
Zone2 & ML1	2.9	41.9	31.6
Zone2 & ML2	3.2	43.4	31.6

The distance attenuation, $D_{2,S}$, and A-weighted SPL at 4m, $L_{p,A,S,4m}$, along ML1 and ML2 in Zone 1, are quite different. For ML1 there is a screen between the source and the first receiver, resulting in a relatively large SPL reduction at the first receiver. For ML2, the receiver has free sight to the source, and the SPL is relatively large. For Zone 1, the furthest microphone position along ML1, and correspondingly the source in ML2 are very close to the wall. This is, as mentioned earlier not in compliance with ISO 3382-3 [2], and might give some unwanted effects. One of these unwanted effects could be that the speaker no longer is as omni-directional for the low frequencies. The same is the case in Zone 2, where both ends of the lines are less than $2m$ from the wall. For Zone 2, the distance attenuation along ML1 and ML2 ought to be quite similar, and it is.

The material parameters and RT in Zone 1 for the two simulation models is very similar. $D_{2,s}$, and $L_{p,A,S,4m}$ are therefore also quite similar.

For Zone 2 there are larger differences in the material parameters and the RT. Simulation model 2 in Zone 2, has a generally lower RT and more absorbent. Hence, one would expect the $D_{2,s}$, and $L_{p,A,S,4m}$ to be lower. The $L_{p,A,S,4m}$ is lower, but the $D_{2,s}$ is not. It seems like the first receiver along both ML gets a relatively low SPL, while the other receivers get strong reflections. From Figure4.3 we can see that the large wall on the left side probably gives strong reflections as it also has low high frequency absorption and low scattering. A couple of tests were done to improve the simulated $D_{2,s}$, but none of them gave improved results. The $L_{p,A,S,4m}$ is much lower for both simulation models than for the measurements. The low $D_{2,s}$ and $L_{p,A,S,4m}$ values, are a strong indication that the SPL at the first receivers is to low for both ML's. Increasing the $L_{p,A,S,4m}$ would increase the $D_{2,s}$, that could be done by increasing the SPL at the first receiver. The measurements source has a diameter of $388mm$, while the simulations are done with a point source. The high of the screens in the office were between $1.25m - 1.45m$ from the floor. It is possible that the highest element on the measurement source had almost free sight to the receiver.

Although the speaker is omni-directional, the individual membranes are directional. The highest membrane is at a height of about $1.4m$ and might have free sight to the receiver. The membrane is not necessarily pointed towards the receiver and the sound from the membrane might be diffracted around the speaker or have directivity due to the direction the membrane is facing. Both the later cases would attenuate the sound, but probably not as much as the screen.

There are many possible reasons why the measured and simulated values differ, more of these reasons will be discussed in the Chapter 6.

5.4 STI based parameters

The STI based parameters (STI in nearest workstation, r_d , r_p). The STI is highly dependent on the background noise level, and "BGN day" is the one closes to the description in ISO 3382-3 [2].

As mentioned earlier, the background noise has a large effect on the STI. Table 5.6 shows the STI based parameters (STI in nearest workstation, r_d , r_p), estimated using "BGN day" and NC25. The STI is estimated using the Matlab function as described in Chapter 4.

Table 5.6: Measured and simulated STI based parameters.

	BGN day			**NC 25**		
Zone & ML	**STI in nearest Work Station**	r_d	r_p	**STI in nearest Work Station**	r_d	r_p
Measured						
Zone 1 & ML1	0.79	10.9	20.7	0.73	7.1	14.8
Zone 1 & ML2	0.80	12.5	21.3	0.73	9.0	15.8
Zone 2 & ML1	0.75	11.2	21.2	0.71	8.1	15.9
Zone 2 & ML2	0,76	10.6	20.2	0.71	7.6	15.2
Simulation method 1						
Zone 1 & ML1	0.75	11.1	25.6	0.65	5.2	16.5
Zone 1 & ML2	0.88	10.1	15.4	0.82	7.9	12.3
Zone 2 & ML1	0.72	12.5	30.8	0.66	6.9	20.4
Zone 2 & ML2	0.69	13.9	34.0	0.61	7.4	23.4
Simulation method 2						
Zone 1 & ML1	0.74	11.3	27.8	0.64	4.9	17.5
Zone 1 & ML2	0.88	9.9	14.9	0.82	7.8	12.1
Zone 2 & ML1	0.72	15.7	45.1	0.59	5.3	27.9
Zone 2 & ML2	0.62	14.3	39.6	0.54	6.2	24.6

From Table 5.6 we see that the STI, r_d and r_p get much lower when the background noise level is higher, using NC25. This was expected. The STI algorithm has frequency weighting NEK EN 60268-16 [5], so if the background noise was very high at the low weighted places it would not necessarily give lower STI.

Figures 5.6-5.8 show the STI versus source-receiver distance along ML 1-2 inn Zone 1. The A-weighted background noise level of daytime has been used, and the figures are plotted according to ISO 3382-3 [2].

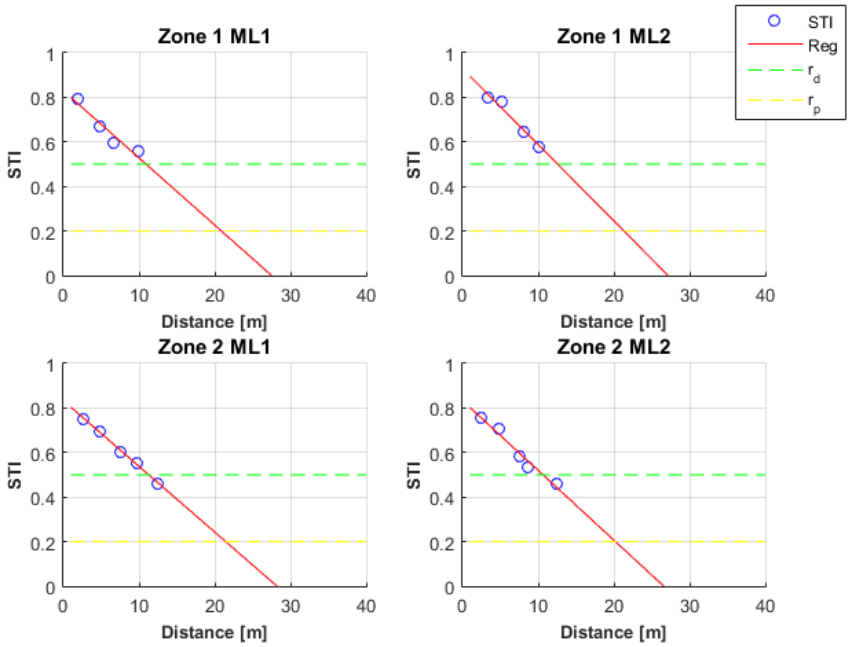

Figure 5.6: Measured STI versus S-R distance.

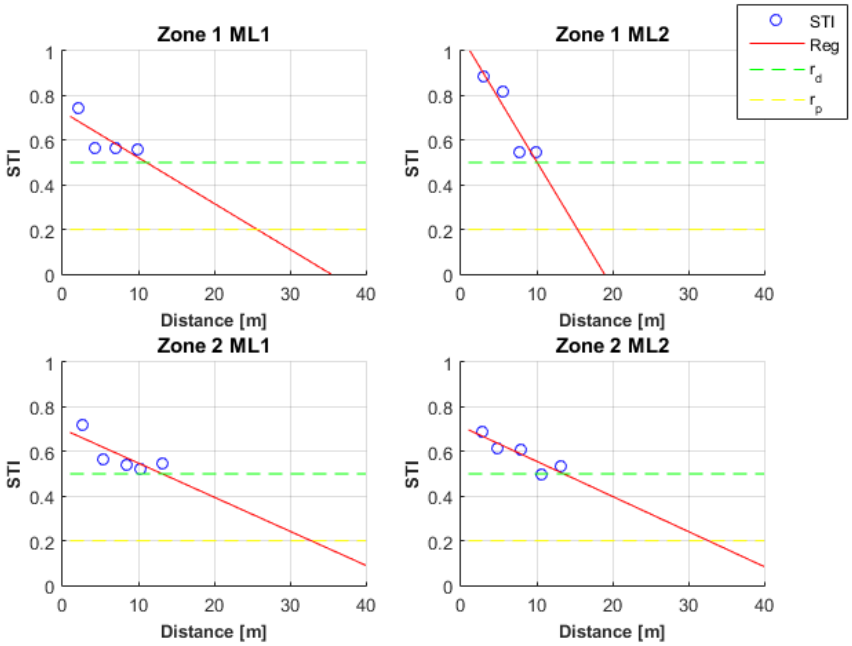

Figure 5.7: Simulation model 1, STI versus S-R distance.

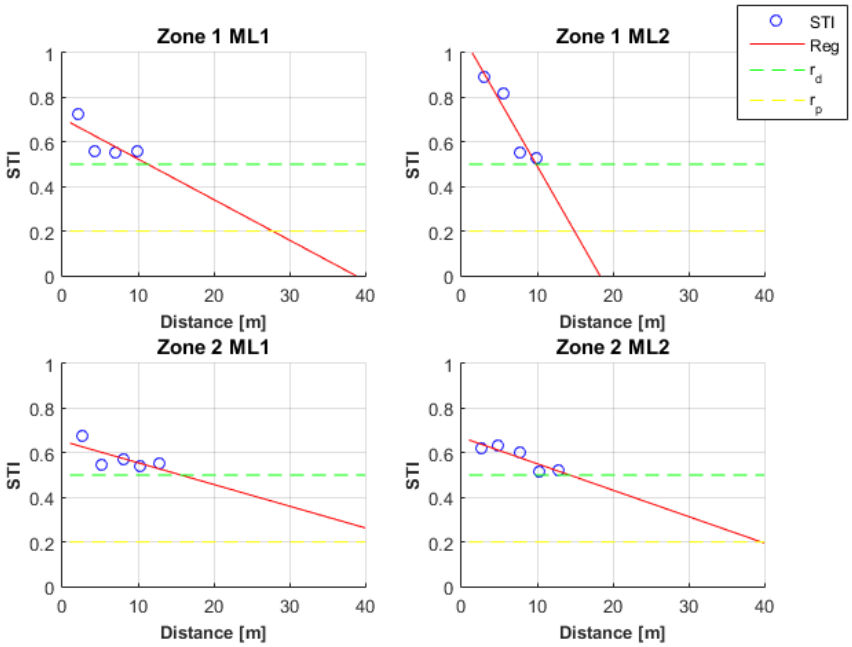

Figure 5.8: Simulation model 2, STI versus S-R distance.

The measured STI for each of the measurement positions decreases almost linearly with the S-R distance. The simulated values do not follow the trend so clearly. The regression analysis indicate lower STI for increased S-R distance. However, the individual simulation results are not consistently estimating lower STI for increased S-R distance.

5.5 Correlation

The correlation between the ISO 3382-3 parameters $D_{2,S}$, $L_{p,S,4m}$, r_d and r_p has been estimated. It was estimated separately for the measurements and each of the simulation models. The correlation analysis was done by comparing the four values attained from Zone 1 and 2 along ML1 and 2.

The values used for estimating the correlations are given in Table 5.7.

Table 5.7: Parameters used in correlation analysis.

Parameter	**Zone1 ML1**	**Zone 1 ML2**	**Zone 2 ML1**	**Zone 2 ML2**
Measured				
$D_{2,S}$	4.6	6.9	7.4	7.2
$L_{p,A,S,4m}$	47.6	51.7	49.0	47.6
r_d	10.9	12.5	11.2	10.6
r_p	20.7	31.3	21.2	20.2
$L_{p,A,B}$	29.2	29.2	31.6	31.6
Simulation model 1				
$D_{2,S}$	3.4	7.8	4.6	3.8
$L_{p,A,S,4m}$	44.7	50.7	44.5	44.1
r_d	11.1	10.1	12.5	13.9
r_p	25.6	15.4	30.8	34.0
$L_{p,A,B}$	29.2	29.2	31.6	31.6
Simulation model 1				
$D_{2,S}$	3.2	7.8	2.9	3.2
$L_{p,A,S,4m}$	44.8	50.9	41.9	43.4
r_d	11.3	9.9	15.7	14.3
r_p	27.8	14.9	45.1	39.6
$L_{p,A,B}$	29.2	29.2	31.6	31.6

Table 5.8 shows the estimated correlation coefficients for the measured values.

Table 5.8: Estimated correlation coefficients from measured values

	$D_{2,S}$	$L_{p,A,S,4m}$	r_d	r_p	$L_{p,A,B}$
$D_{2,S}$	1	-	-	-	-
$L_{p,A,S,4m}$	0.37	1	-	-	-
r_d	0.20	0.99	1	-	-
r_p	0.16	0.79	0.80	1	-
$L_{p,A,B}$	NA	NA	-0.55	-0.34	1

The results for the measurements indicate little to no correlation between the $D_{2,S}$ and the other parameters, and between $L_{p,A,B}$ and r_d, r_p. They indicate a strong positive correlation between $L_{p,A,S,4m}$ and r_d, r_p, and between r_d and r_p. Table 5.9 shows the estimated correlation coefficients for the values from simulation model 1.

Table 5.9: Estimated correlation coefficients from simulation model 1.

	$D_{2,S}$	$L_{p,A,S,4m}$	r_d	r_p	$L_{p,A,B}$
$D_{2,S}$	1	-	-	-	-
$L_{p,A,S,4m}$	0.96	1	-	-	-
r_d	-0.64	-0.78	1	-	-
r_p	-0.83	-0.93	0.95	1	-
$L_{p,A,B}$	NA	NA	0.91	0.84	1

Table 5.10 shows the estimated correlation coefficients for the values from simulation model 2.

Table 5.10: Estimated correlation coefficients from simulation model 2.

	$D_{2,S}$	$L_{p,A,S,4m}$	r_d	r_p	$L_{p,A,B}$
$D_{2,S}$	1	-	-	-	-
$L_{p,A,S,4m}$	0.97	1	-	-	-
r_d	-0.75	-0.89	1	-	-
r_p	-0.87	-0.96	0.98	1	-
$L_{p,A,B}$	NA	NA	0.95	0.90	1

The results indicate the same trend for both simulation models, this is expected as they have the same physical model. There is a strong negative correlation between $D_{2,S}$ and r_d, r_p, and between $L_{p,A,S,4m}$ and r_d, r_p. A strong positive correlation between $D_{2,S}$ and $L_{p,A,S,4m}$, and between $L_{p,A,S,4m}$ and r_d, r_p. r_d and r_p also have a strong positive correlation.

There is observed a large difference between measured and simulated parameter values with respect to correlation strength and positive versus negative correlations. The correlation is estimated from four parameters which might not be enough to fully trust the results.

Table 5.11 shows the correlation between parameters measured in 16 different offices by Virjonen et al. [29]. Only offices number 1, 3-5, 7-13 and 15 are open-plan offices.

Table 5.11: Correlation between different acoustic parameters of 16 different offices, Virjonen et al. [29]

Parameter	DL_2 **[dB]**	$L_{p,S,4m}$ **[dB]**	DL_f **[dB]**	T_{20} **[s]**	EDT **[s]**	r_p **[m]**	$L_{p,B}$**[dB]**
DL_2 **[dB]**	1	-	-	-	-	-	-
$L_{p,S,4m}$ **[dB]**	-0.65	1	-	-	-	-	-
DL_f **[dB]**	-0.83	0.9	1	-	-	-	-
T_{20} **[s]**	-0.33	0.37	0.44	1	-	-	-
EDT **[s]**	0.11	0.06	0.10	0.82	1	-	-
r_p **[m]**	-0.47	0.62	0.62	-0.13	-0.47	1	-
$L_{p,B}$**[dB]**	NA	NA	NA	NA	NA	0.10	1

The parameters DL_2, $L_{p,S,4m}$ and $L_{p,B}$ are a similar parameter to $D_{2,S}$, $L_{p,A,S,4m}$ and $L_{p,A,B}$ in my study. The parameters in my study are A-weighted while the ones in Virjonen et al. [29] are not. The A-weighting does not effect the correlation as it changes the parameters by a constant factor. The correlation on the measured results in Table 5.8 do not support the finding of Virjonen et al. [29].

Chapter 6

Special study on Diffraction

In this Chapter, the estimation of diffraction using Odeon, Catt and a Matlab toolbox will be studied. The diffraction around a thin and a thick hard screen on a hard floor with no air absorption and 100% absorbent walls and ceiling is studied.

First the methods for estimating the diffraction is shown. Then a validation/reasoning for choosing EDB1 over ESIE is done. Then three comparisons are shown. Source position 1 (S_1) and receiver positions 1 (R_1) , 7 (R_7) and 16 (R_{16}) are used for comparison. The first is a comparison for the diffraction estimated using first order diffraction (d) and second order diffraction (dd), Odeon, CATT and EDB1 will be compared. The second comparison is for the full estimation using CATT and second order diffraction using EDB1. The third is for full estimation versus the d and dd estimation using CATT and EDB1.

The Matlab toolboxes estimate d, Sd, dS, SdS and dd. CATT estimates d, Sd, dS and dd, while Odeon only estimates d or dd, depending on the case. Figure 6.1 shows these paths over the top of the screen (z-axis).These six paths are likely to represent the largest peaks on the impulse responses. There is also diffraction along the sides of the screen.

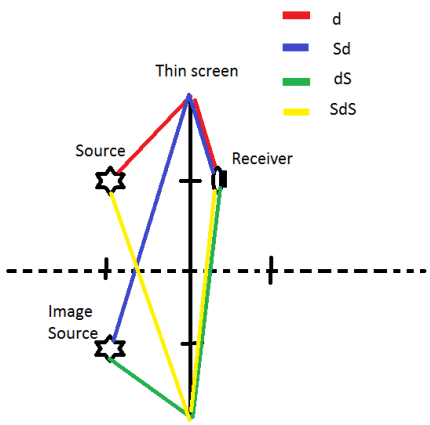

Figure 6.1: Paths over screen d, Sd, dS and SdS paths.

6.1 Method

The setups are composed of a thin and a thick screen on a hard floor with absorbent walls. The screens are $2m$ high, $4m$ wide and $0m$ and $0.5m$ thick, respectively. Two source positions, with height $1m$ above the floor, and $1m$ and $2m$ away from the screen, in the -y-direction are used. 22 receivers for the thin screen and 23 for the thick screen were used. The first 10 receivers were at the same height as the sources, and spaced $0.1m$, $0.5m$, $1m$ and then with $1m$ steps from $1m - 8m$, along the +y-axis. The next 12 and 13 receivers were distributed as shown in Figure 6.2b and Figure6.3b, respectively. They had a distance of $3m$ from the center of the screen at height $1m$, starting at $5°$ for the thin screen and $0°$ for the thick screen between the y-axis and z-axis, increasing by steps of $5°$ up to $60°$. Note that the S-R distances will be different for the thin and the thick screen.

6.1.1 CATT and Odeon analysis

A square room with $20m$ long sides was modeled, and a screen was placed on the floor in the center of the room (i.e. the center of the x- and y-axis). This was done with a thin and a thick screen of $0m$ and $0.5m$ thickness, respectively. The width and height of the screen were $4m$ and $2m$,respectively. The walls were given absorption coefficients of 0.999 in CATT and 100% in Odeon, i.e. total absorption. The floor and screen were both given absorption coefficients of 0 for both, i.e. total reflection. The scattering was set to zero for all planes in CATT and for all materials in Odeon. The sources and receivers were placed as described above. The layout is shown in Figure 6.2 - 6.3. The source and receiver were both set to be omni-directional. In CATT, the source was set to produce a $94dB$ white noise signal at $1m$, while it was set to produce a Sound Power Level of $0dB$ in Odeon. Since simulation is done noise free, the levels do not matter, other than for attaining relative levels. Measurements in CATT were stored relative to free field at $1m$.

To attain the same in Odeon, $11dB$ had to be added to the measured levels.

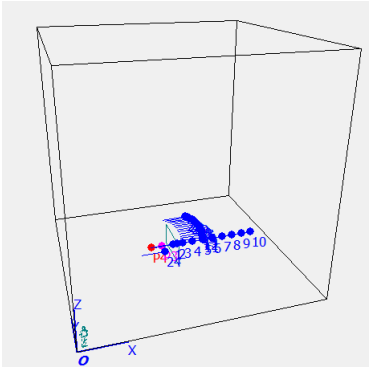

(a) The screen, source positions (red) and receiver positions (blue) plotted using Odeon.

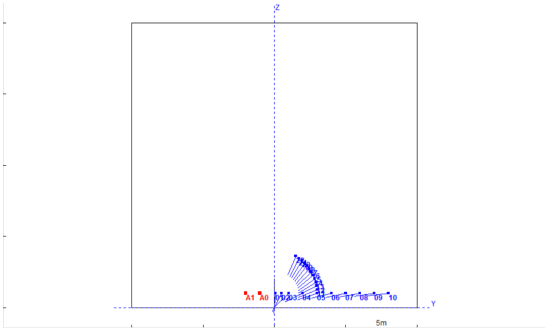

(b) The screen, source positions (red) and receiver positions (blue) plotted using CATT PL9Viewer.

Figure 6.2: Layout with thin screen.

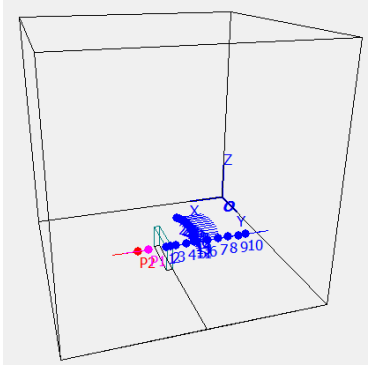

(a) The screen, source positions (red) and receiver positions (blue) plotted using Odeon.

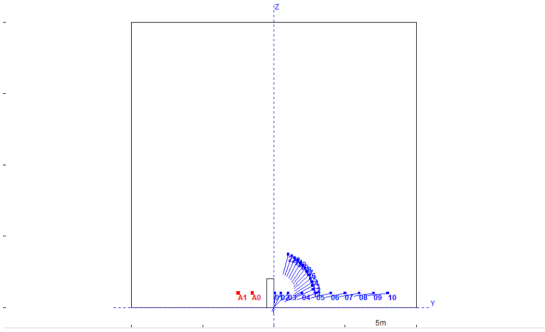

(b) The screen, source positions (red) and receiver positions (blue) plotted using CATT PL9Viewer.

Figure 6.3: Layout with thick screen.

For CATT, in the ”SxR prediction”, a $0.5s$ long impulse response was chosen, along with 0 rays. By choosing 0 rays, only the diffraction is estimated. The air absorption was turned off.

Two types of estimations were done. One using $1st$ and $2nd$ order diffraction, and the other with all diffraction on, that means d, Sd, dS and dd.

For Odeon, in the ”SxR prediction”, a $0.5s$ long impulse response was chosen, along with 1 ray. 0 rays was not a possible input. Estimations was done with screen diffraction on. The air absorption was turned off.

I would like to give the following remarks as lessons learned. At first I though a high number of rays was needed, such that the ray would hit a point, a ”hit-box”, that

corresponded to the diffraction path to the receiver. In hindsight I found out that the diffraction is estimated separately, and is independent of the number of rays. If we chose to use a large number of rays the 100% absorbent walls would ensure that the walls absorb all incoming sound. When using 0 rays, the absorption of the walls does not matter, since no sound is emitted, but the absorption of the screen and floor are important as they are inputs for the diffraction estimation. The absorption on the floor would attenuated the images source and absorption on the screen would attenuate the diffracted sound.

It is possible to obtain a neutral impulse response in Odeon, which is the same as one would obtain with a microphone during a measurement. But even when no HRTF is used, filtering is still applied. Since all calculation in Odeon are in the energy domain, artificial phase is added to make the energy-based impulse response look like a pressure (real) impulse response. Therefore, an impulse response obtained in Odeon will never look like a real impulse response measurement in detail. The overall energy behavior will be the same, but reflections might vary a lot, Odeon User Manual [9].

When no direct sound is received from a point source at a receiver position, Odeon will try to detect a one- or two-point diffraction path. Odeon uses the algorithms suggested by Pierce [24]. By only calculating the diffracted contribution when the point source is not visible, the contribution can be added to the impulse response without considering the phase-interaction between direct sound and the diffracted component, just like the reflections are added to the impulse response. Only diffraction from one edge of the diffracting object is taken into account, the one with the shortest path-length. The edge of diffraction is considered infinitely long. More information and validation is found from Rindel et al. [25].

”Odeon is capable of handling more complicated objects than the single surface screen, e.g. objects such as book shelves, the corner in e.g. a L-shaped room and buildings outdoors or diffraction over a balcony front edge or over the edge in an orchestra pit.”, Odeon User Manual [9].

6.1.2 Matlab analysis

Instead of using a hard floor, the height of the wall was doubled to $4m$, and a image sources was used at the image positions of the two sources, resulting in a total of 4 sources. The same source and receiver positions as describe earlier were used. The combined values for source $1-2$, source $3-4$ represent source 1 and source 2, respectively. Figure 6.4 shows the screens, the source positions (blue X) and the receiver positions(red O).

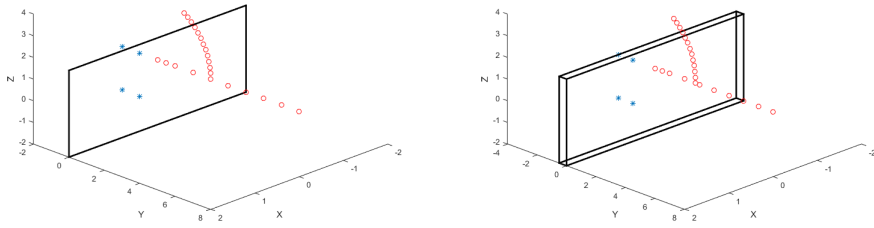

(a) The thin screen.

(b) The thick screen.

Figure 6.4: Thin and thick screens with source positions and receiver positions plotted using the toolboxes plotting function (ESIE1plotmodel). The blue X marks are the source positions, and the red O are the receiver positions.

The diffraction was estimated using two different toolboxes, ESIE1 and EDB1, Peter Svensson [27]. The diffraction for the low frequencies, $63Hz - 1kHz$ octave bands, was estimated using the ESIE1 toolbox. This toolbox estimates in the frequency domain, and is integral equation-based. For this toolbox the diffraction was set using "inteqsettings.niterations = 0", resulting in $1st$ and $2nd$ order computations, stored as "tfdiff" and "tfineqdiff". The frequency and number of edge elements are linearly dependent. Figure 6.5 shows the relationship. Using more than 60 edge elements results in a very long computation time, therefore it was set to 40, so that it is accurate up to the $1kHz$ octave band.

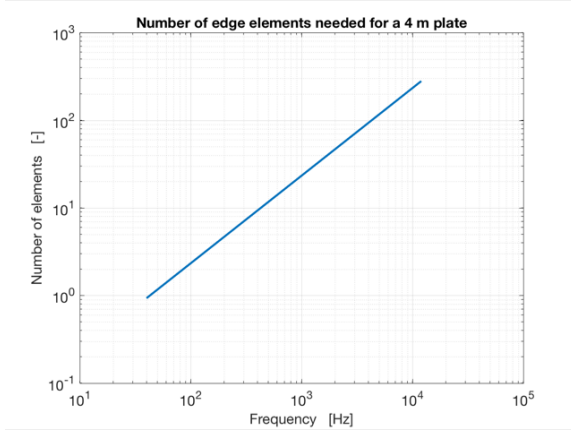

Figure 6.5: Number of edge elements needed to accurately calculate the diffraction vs frequency, Svensson P. [26].

The diffraction for the $63kHz - 8kHz$ octave bands was estimated using the EDB1 toolbox, which estimates in the time-domain, and is iterative, see Peter Svensson [27].

For this toolbox, the diffraction was set to $1st$ and $2nd$ order estimations. Higher order estimation is possible, but demands a lot of computational power and takes a long time.

6.2 Comparing results from EDB1 and ESIE

The results using the ESIE1 toolbox were stored as transfer functions, with resolution of 250 points between $40hz$ and $1500Hz$. The EDB1 toolbox results were stored as impulse responses with sampling frequency $44.1kHz$.

A comparison between ESIE1 and EDB1 was done to see whether the EDB1 toolbox was good enough to estimate the $1st$ and $2nd$ order diffraction with the thick and thin screen from $63kHz - 8kHz$ octave band range. The frequency responses using the thin screen and $1st$ and $2nd$ order diffraction are close to identical when estimating using ESIE1 and EDB1. Figures 6.6-6.7 show some examples.

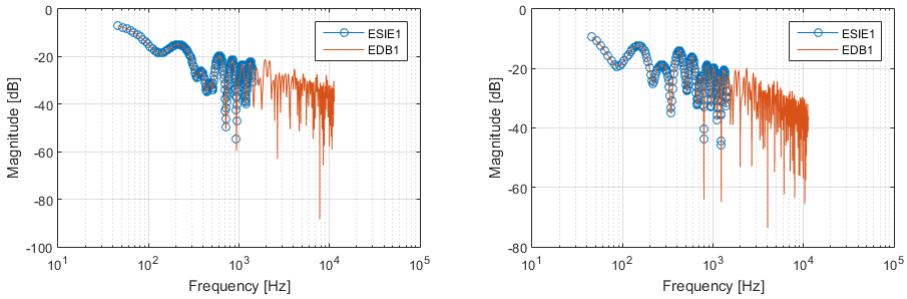

(a) FR, S_1 and R_5.

(b) FR, S_1 and R_{15}.

Figure 6.6: EDB1 vs ESIE1, FR with thin screen $1st$ order diffraction, S_1 and R_1 and R_{15}.

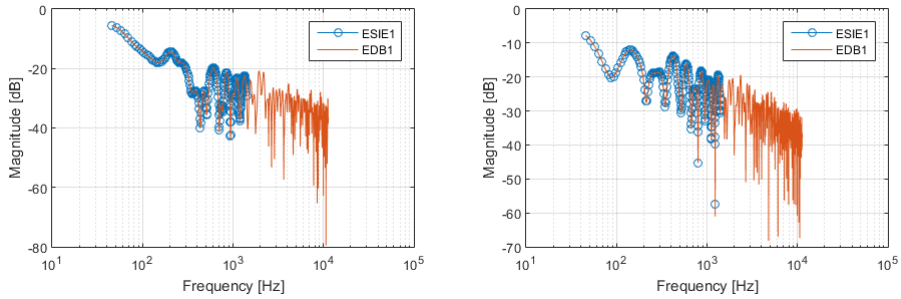

(a) FR, S_1 and R_5.

(b) FR, S_1 and R_{15}.

Figure 6.7: EDB1 vs ESIE1, FR with thin screen $2nd$ order diffraction, S_1 and R_1 and R_{15}.

When using the thick screen, the frequency responses is minus infinity (-inf) for all receivers below receiver 14, 15°, when using $1st$ order diffraction. But for receivers 15

and above, results from EDB1 and ESIE1 seem to be close to identical, Figure 6.8 shows and example. When using $2nd$ order diffraction they also fit very well, except for position 15 between the $200 - 500Hz$. Figure6.9 show the worst fit at position 15 and a regular fit at position 5.

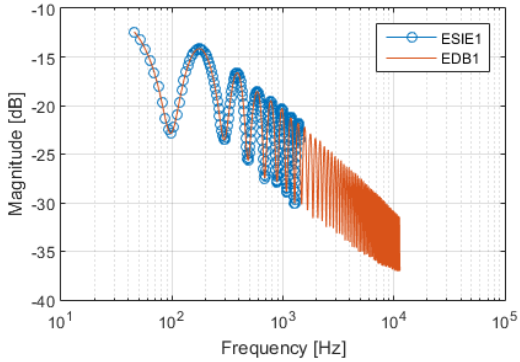

Figure 6.8: ESIE1 vs EDB1, FR with thick screen and $1st$ order diffraction, S_1 and R_{15}.

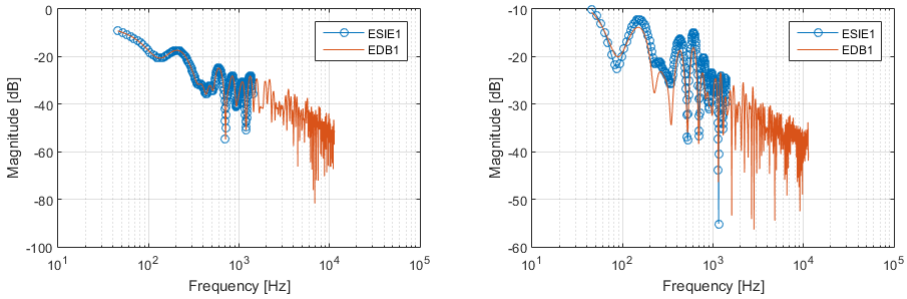

(a) FR, S_1 and R_5.

(b) FR, S_1 and R_{15}.

Figure 6.9: EDB1 vs ESIE1, FR with thick screen, $2nd$ order diffraction, S_1 and R_1 and R_{15}.

From this it is concluded that the ESIE1 and EDB1 are close enough to go ahead and only use the EDB1 toolbox. It has the advantage of calculating in the time domain, thus providing impulse responses and higher frequency resolution. At the same time it is very close to the more accurate but lower frequency resolution results from ESIE1.

The next step is then to check how close the $2nd$ order calculation are to higher order calculations. The $15th$ order diffraction was estimated using the ESIE1 toolbox for the thin and thick screen. The higher order calculation do not seem to give a much better precision, they are very close to the $2nd$ order calculation. Figure **??** shows the thin screen and Figure 6.11 shows the thick screen.

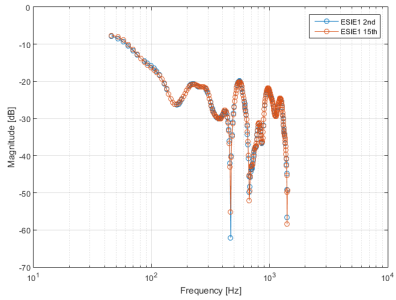

(a) FR, S_1 and R_7.

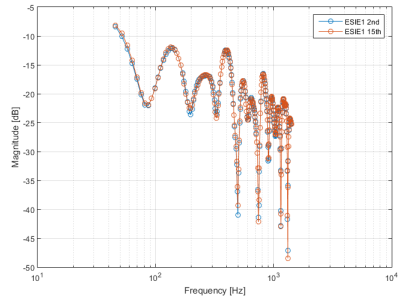

(b) FR, S_1 and R_{16}.

Figure 6.10: ESIE1, FR using thin screen, $2nd$ and $15th$ order diffraction, S_1 and R_7 and R_{16}.

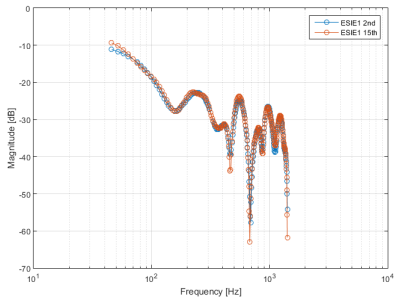

(a) FR, S_1 and R_7.

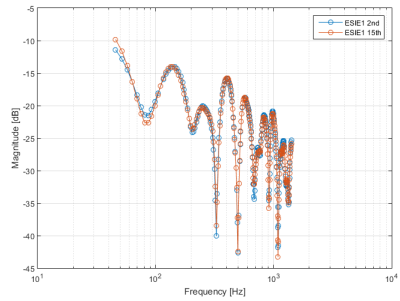

(b) FR, S_1 and R_{16}.

Figure 6.11: ESIE1, FR using thick screen, $2nd$ and $15th$ order diffraction, S_1 and R_7 and R_{16}.

6.3 1. and 2. order diffraction results with Odeon, CATT and EDB.

Odeon calculates diffraction as either d or dd. In this section a comparison of the diffraction estimated using first and second order diffraction, d and dd for the two simulation tools and the Matlab script EBD1 was done. In Odeon, screen diffraction was turned on. In CATT d and dd was turned on, while Sd and dS was turned off. For EDB1, only the source, not the image source was used, and a rectangular filter to remove SdS was used. The IR in Odeon is not comparable with the ones attained using CATT and EDB1, and will not be shown. Figures 6.12- 6.14, show the IR and FR simulated using a thin screen with S_1 and 3 different receiver positions. These are positions R_1, R_7 and R_{16}. R_1 is the one closest to the screen, $0.1m$ away from the center. R_7 is the on $5m$ away from the center of the screen, and R_{16} is $3m$ away from the center of the screen at an angle of $30°$ for the thin screen and $25°$ for the thick. The same positions are used from herein and throughout this

Chapter. The FR is estimated in 1/1 octave band values. The IR for Odeon is not shown and will be explained later. For the IR figures, ”edb” denotes calculations with EDB1.

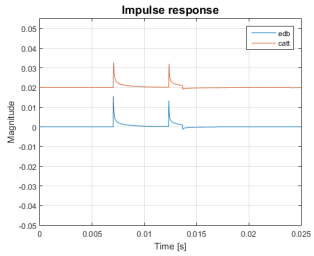

(a) IR, S_1 and R_1.

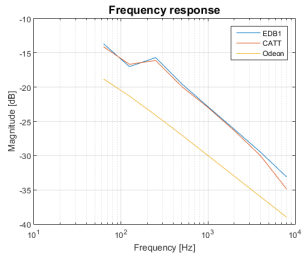

(b) FR, S_1 and R_1.

Figure 6.12: Odeon, CATT and EDB1, IR and FR thin screen, S_1 and R_1.

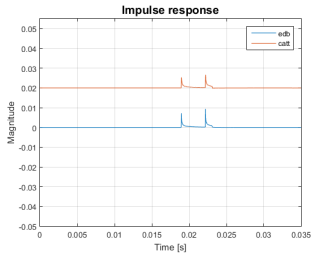

(a) IR, S_1 and R_7.

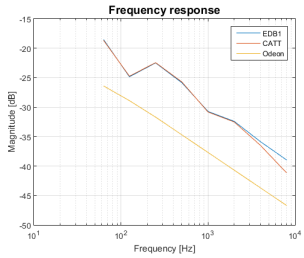

(b) FR, S_1 and R_7.

Figure 6.13: Odeon, CATT and EDB1, IR and FR thin screen, S_1 and R_7.

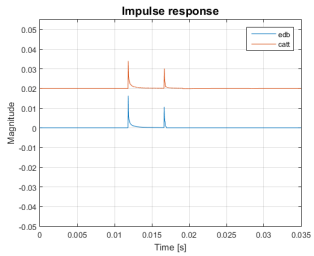

(a) IR, S_1 and R_{16}.

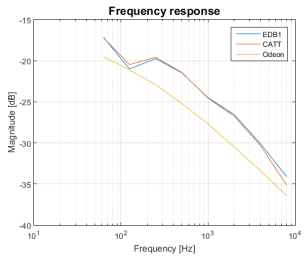

(b) FR, S_1 and R_{16}.

Figure 6.14: Odeon, CATT and EDB1, IR and FR thin screen, S_1 and R_{16}.

The IR and FR are close to identical for EDB1 and CATT. The FR estimated in Odeon is several dB lower than the other two, except at R_{16}. The FR in Odeon is dB linear for all three positions.

Figures 6.15- 6.17, show the IR and FR simulated using a thick screen.

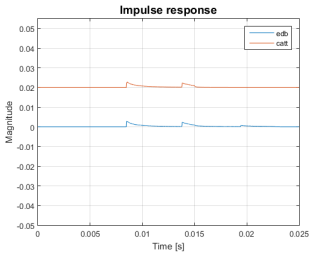

(a) IR, S_1 and R_1.

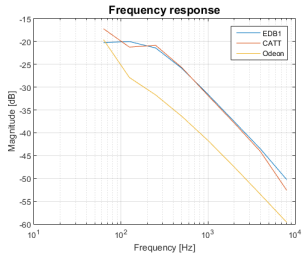

(b) FR, S_1 and R_1.

Figure 6.15: Odeon, CATT and EDB1, IR and FR thick screen, S_1 and R_1.

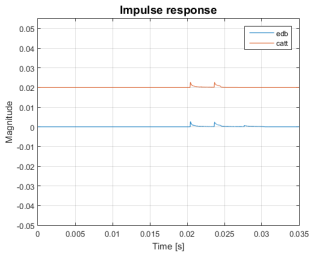

(a) IR, S_1 and R_7.

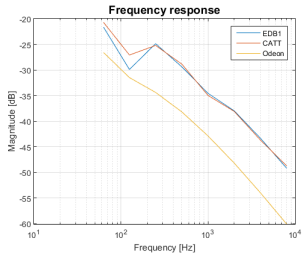

(b) FR, S_1 and R_7.

Figure 6.16: Odeon, CATT and EDB1, IR and FR thick screen, S_1 and R_7.

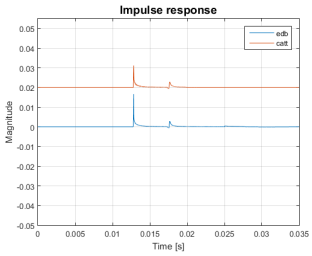

(a) IR, S_1 and R_{16}.

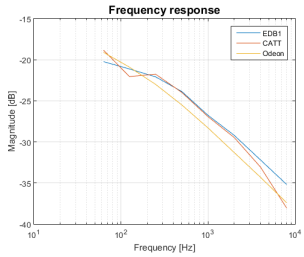

(b) FR, S_1 and R_{16}.

Figure 6.17: Odeon, CATT and EDB1, IR and FR thick screen, S_1 and R_{16}.

The IR and FR are slightly different for EDB1 and CATT, but they are still very similar. The FR estimated using Odeon is still very much lower than for the two other tools, except for at R_{16}.

A test was done to see where the FR in Odeon was similar to the others. It turned out too be for R_{15}, R_{17} and R_{18}. Figures of these and other positions are shown in Appendix B.1. The same can be seen for S_2 at the same receiver positions, these results along with others are shown in Appendix B.2.

6.4 Complete diffraction estimation with CATT and EDB1.

This section contains a comparison off the complete $2nd$ order estimation using CATT and EDB1. In CATT, d, Sd, dS and dd were on. In EDB1, the source and image source were used, and $2nd$ order estimation was chosen. Figures 6.18 - 6.20 show the IR and FR for 1/1 octave bands.

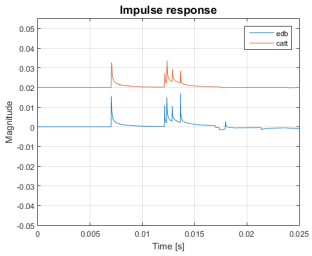

(a) IR, S_1 and R_1.

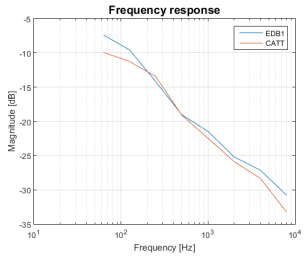

(b) FR, S_1 and R_1.

Figure 6.18: Complete estimation using CATT and EDB1, IR and FR thin screen, S_1 and R_1.

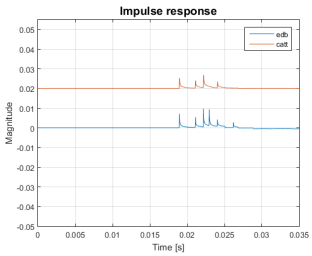

(a) IR, S_1 and R_7.

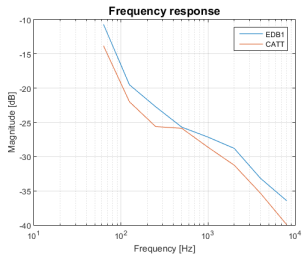

(b) FR, S_1 and R_7.

Figure 6.19: Complete estimation using CATT and EDB1, IR and FR thin screen, S_1 and R_7.

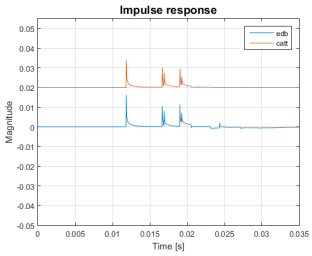

(a) IR, S_1 and R_{16}.

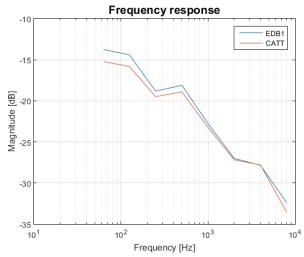

(b) FR, S_1 and R_{16}.

Figure 6.20: Complete estimation using CATT and EDB1, IR and FR thin screen, S_1 and R_{16}.

IT can be seen from the figures that the impulse response and frequency response

are quite similar. The impulse responses for EDB1 has an extra peak at the end that corresponds to the SdS, which CATT does not model. After conversation with Bengt-Inge Dalenbeck [11], the developer of CATT, he said that not modeling the SdS component was a conscious decision as it will not have much effect on the accuracy of the estimation. The peaks in the IR's are at the same places, but have somewhat different amplitudes. From Figure 6.19a peak number 4 for EDB1 is not present in CATT. The FR's are very similar, and deviate by $3dB$ at the most.

Figures 6.21 show the FR for all frequencies at R_7 and R_{16}.

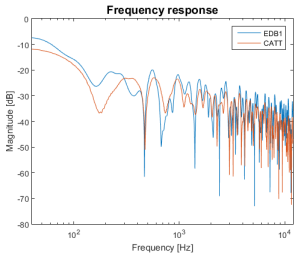

(a) FR, S_1 and R_7.

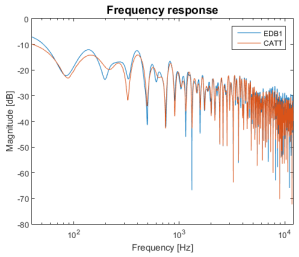

(b) FR, S_1 and R_{16}.

Figure 6.21: Complete estimation using CATT and EDB1, FR thin screen, S_1 and R_7 and R_{16}.

For both positions, the FR's have a very similar pattern. And from the octave band values we see that they are very similar.

Now we try with the thick screen. The same source and receiver positions are used and shown in Figures 6.22-6.24. The FR is now in 1/1 octave band values.

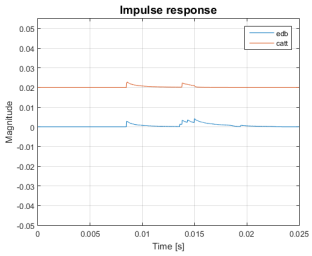

(a) IR, S_1 and R_1.

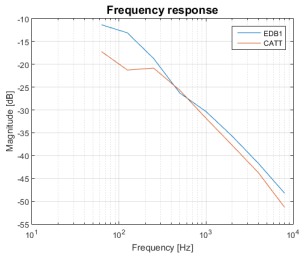

(b) FR, S_1 and R_1.

Figure 6.22: Complete estimation using CATT and EDB1, IR and FR thick screen, S_1 and R_1.

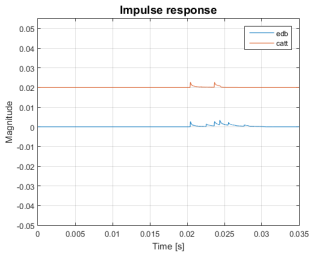

(a) IR, S_1 and R_7.

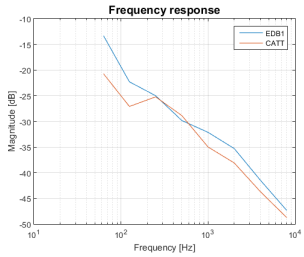

(b) IR, S_1 and R_7.

Figure 6.23: Complete estimation using CATT and EDB1, IR and FR thick screen, S_1 and R_7.

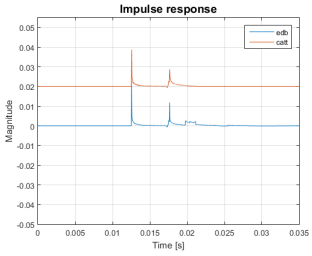

(a) IR, S_1 and R_{16}.

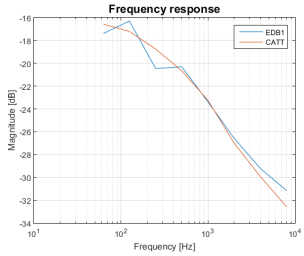

(b) FR, S_1 and R_{16}.

Figure 6.24: Complete estimation using CATT and EDB1, IR and FR thick screen, S_1 and R_{16}.

There is more detail in the IR's attained using EDB1, than CATT. The FR's have largest deviation in the low frequencies, 63-250Hz.

Figures 6.21 show the FR for all frequencies, but only for position 1 and 16.

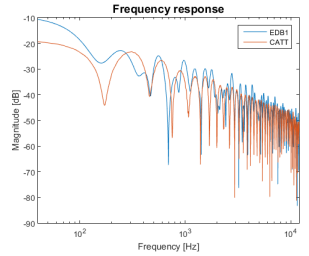

(a) FR, S_1 and R_7.

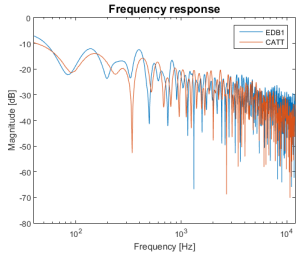

(b) FR, S_1 and R_{16}.

Figure 6.25: Complete estimation using CATT and EDB1, FR thick screen, S_1 and R_7 and R_{16}.

The results are similar as for the thin screen.

6.5 Comparing CATT and EDB1 results with complete diffraction versus 1. and 2. order diffraction

Now we look at the complete estimation versus $1st$ and $2nd$ order diffraction using CATT and EDB1, shown in Figures 6.26 - 6.28.

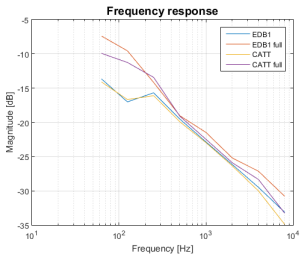

(a) FR thin screen, S_1 and R_1.

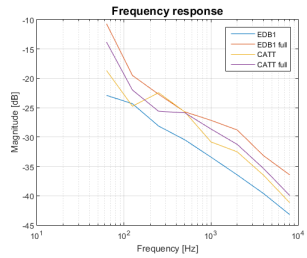

(b) FR thin screen, S_1 and R_7.

Figure 6.26: Complete vs 1. and 2. order estimation using CATT and EDB1, FR thin screen, S_1 and R_1 and R_7.

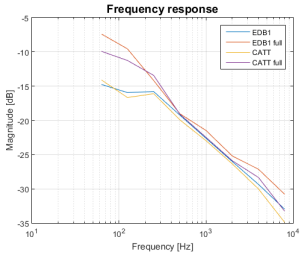

(a) FR thin screen, S_1 and R_{16}.

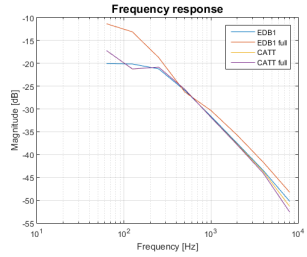

(b) FR thick screen, S_1 and R_1.

Figure 6.27: Complete vs 1. and 2. order estimation using CATT and EDB1, FR thin and thick screen, S_1 and R_{16} and R_1.

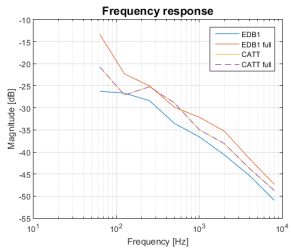

(a) FR thick screen, S_1 and R_7.

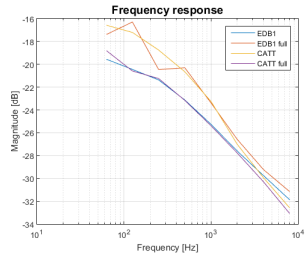

(b) FR thick screen, S_1 and R_{16}.

Figure 6.28: Complete vs 1. and 2. order estimation using CATT and EDB1, FR thick screen, S_1 and R_7 and R_{16}.

The $63Hz - 250Hz$ octave band have the largest deviation between the complete estimation of diffraction and the $1st$ and $2nd$ order estimation. From Figure 6.26b and Figure 6.28a the lower than the others. For the other Figures except Figure 6.28b the estimation using complete diffraction and $1st$ and $2nd$ order diffraction are quite similar, especially from $500Hz$ and below.

6.6 Conclusion

EDB1 simulates diffraction with high accuracy, and provides detailed results. Simulations using EDB1 are very time consuming and require a lot of computational power. Diffraction simulation using CATT is much faster, but loses some details. Simulations of diffraction using Odeon is very fast, but a little detail in the results.

Assuming that EDB1 is the closest to the reality, we can see that CATT estimates the diffraction very well. We can also conclude that Odeon in many cases strongly underestimates the diffraction. Odeon ought to try to simulate diffraction in more detail as it can have strong effects. Odeon might adjust for this in other ways, which I have not investigated. Using both S_1 and S_2, Odeon is closest to EDB1 and CATT for receiver positions 15-18, showed in Appendix B.

Chapter 7

Discussion

This Chapter extends the discussion done in Chapter 5, elaborates some important sources of uncertainty and propose recommendations for extended work.

Some of the uncertainties in the measurements are due to the sensitivity in regards placement of the speaker and receiver in the room. Measurements were done closer to the wall than recommended by the ISO 3382-3 [2]. The whole sphere speaker had a large diameter and is composed of multiple directional membranes.

Uncertainties in the simulations are mostly related to modeling of input data, such as the absorption and scattering coefficients. Room parameters such as temperature and humidity, that effect the air absorption are not measured, which implies uncertainty in the simulations. Modeling of room dimensions and placement of screens, desks, windows, etc. do also impact the results. The number of rays used for estimation, is also a source of uncertainty. Another source of error was using a point source (not physically possible) rather than modeling the actual source.

Assessment of the acoustics in existing buildings is often done by measuring the RT, and then fitting the simulated RT to the measured. Fitting the simulated RT to the measured is difficult as the exact absorption and scattering coefficients usually are uncertain. A large part of the material absorption and scattering choices are based on experience and known measures.

Using the measurement positions along ML1 for Zone 1 and Zone 2, when estimating RT, might not have been a wise choice. Alternatively, one could have used more positions at random height and positions throughout the room, this would ensure that positions with large variations from the mean would have less effect on the total result.

The uncertainty of the absorption coefficient can be very large, see Appendix D.6. Hence, two simulation models are used, with different absorption coefficients to assess the impact. The results from simulation model 1 and 2 show the same trend, although with different specific values for the parameters.

For Zone 2 ML1 and 2, simulated $D_{2,S}$ and $L_{p,A,S,4m}$ are much lower than the measured. This could be due to strong reflections of the wall on the right side of the model, Figure 4.3. One would expect to see the same trend for the measurements, unless the wall

had a larger scattering or more absorption then simulated. The wall had some posters that might have given a bit more absorption for the low frequencies, and maybe a bit larger scattering for the high frequencies, but the biggest area of the wall was clean. A magazine shelf was also present, but not simulated. When looking more closely at the $L_{p,A,S,n}$ parameters from Table 5.4, we see that the simulated $L_{p,A,S,n}$ is much lower for the two first receiver positions. The other positions 3-5 are very close to the measured. This would indicate that the problem is not the reflections from the wall, but that there is a too large sound reduction at the two first receivers. Simulation model 1 has higher RT in Zone 2 than simulation model 2, and $D_{2,S}$ is higher for simulation model 1, which indicates the same.

From the $L_{p,A,S,n}$ parameters in Table 5.4 we also see that when the simulation has direct sound, as for Zone2 ML2 measurement position 1. The simulated $D_{2,S}$ gets much more similar to the measured. It seems likely that a large error lies in the source. The measurements are likely to have direct sound for Zone 1 ML1, and Zone 2 ML1 and ML2, while the simulations do not.

A possible solution would be to lower the screen height between the first receivers or increase the height of the source. Lowering the screens would be altering the office, while increasing the source height is in conflict with ISO 3382-3 [2]. Alternatively one could try to model the Whole sphere source in Odeon. Another possibility would be to set partial transparency on the screens, allowing some of the sound to pass through. One could also reduce the absorption of the screens and possibly model chairs to keep the RT in the same range. The simulated source is $0.05m$ lower than the screen. The problem is that the screen have a high absorption and unless there is free sight between the source and receiver there will be a large reduction, due to the way diffraction is implemented in Odeon. The diffraction component is underestimated, as discussed in Chapter 6. One could try to make a model giving the screen a thickness and lowering the absorption coefficients at the top part of the screen to compensate for the diffraction calculation.

For the simulation, the height of the workstations is $1.25m$ and the source and receivers are point sources placed at a height of $1.2m$. For the measurements, the workstations had different heights, the heights were between $1.25m$ and $1.45m$. The whole sphere speaker had a diameter of $0.388m$ and the center of the speaker was placed at height $1.2m$, thus the highest membrane on the speaker was at a height of about $1.4m$.

A couple of tests to lower the SPL at the center receiver positions were done. One of them was increasing the height of the screen by $0.2m$. Doing so, $D_{2,s}$ was improved by about $2dB$ at ML1, but got worse by about $1dB$ for ML2. Another test was adjusting the scattering of the largest plain wall on the left side of Figure 4.3. The scattering for this wall was 0.04. Attempt with scattering of 0.01, 0.07 and 0.3 were made. However, there was no improvement of the $D_{2,s}$. Another test was to move the source $0.2m$ closer to the desk, and all receivers $0.25m$ closer to the desks. For the measurements, the source was about $0.60m$ away from the desk, and the receivers were about $0.50 - 0.6m$ away from the desks. This made the receiver $0.52m$ away from the desk, and the source $0.55m$ away from the desks in the simulation. This had some effect on the RT, the uncertainty got lower for the higher frequencies. But it had no effect on the $D_{2,s}$.

Other possible solution would be to make the model more detailed, include more objects and use the exact heights of the screens. In addition, one could try to compensate for

the diameter of the whole sphere source, or model it. Including many small details in the model is usually not recommended as it can give strong and unnatural reflections.

A test to see that the parameters estimated using the Matlab script were correct was also done. The estimation of the $D_{2,s}$, $L_{p,A,S,4m}$ and $L_{p,A,B}$ parameters were the same when using Odeon as for the Matlab script, see Appendix A.2.

For the room to be in Class C of the NS 8175, the $D_{2,s}$ has to be $>= 7$, the $L_{p,A,S,4m}$ has to be $<= 52$, BGN has to be $<= 33$, and the r_d should be >=11. The "BGN day" was used to see how well the measured and simulated values fulfill the standard. The background noise fulfills Class C. The $L_{p,A,S,4m}$ fulfills Class C or better for all. The $D_{2,s}$ only fulfills Class C for the measurements in Zone 2 and the simulation in Zone1, ML2. The r_d Class C is fulfilled for the measurements in Zone1 ML1 and Zone 2 ML2. And in simulation model 1 for Zone 1 ML2 and in simulation model 2 for Zone 1 ML2. Otherwise, the r_d is in class D. For a open-plan office to reach a higher Class A or B, it seems as it would be wise to have free field between the source and closest receiver, which could be done with square workstations.This would give a lower, $D_{2,s}$, $L_{p,A,S,4m}$ and a higher STI at the closest receiver, resulting in a shorter r_d.

Further work would be finding an appropriate way for modeling/simulating the source. Angle dependent absorption is important when modeling room that are not diffuse field cases. Therefore, conducting a special study on angle dependent absorption would also be a recommended next step.

Chapter 8

Conclusion

Simulating an Open-plan office present numerous challenges. The material absorption and scattering coefficients are often unknown, and it take practice and experience to get it right. The reverberation time is very hard to adjust in the simulation above $2kHz$. Hence, low scattering seems to result in lower RT and vice versa. The diameter of the sound source and whether or not there could be direct or partially direct sound has to be taken into consideration. The distance attenuation parameters, $D_{2,S}$ and$L_{p,A,S,4m}$ in Zone 1 fit better than for Zone 2. Getting a correct SPL at the early receivers is very important as it has a large impact on these parameter values.

Measurement uncertainty due to limited number of source and receiver positions and their placement are important. Uncertainties due to dimensions of the speaker could be addressed by using a second source to assess differences. The measured data indicate that the office does not have good acoustics, see ISO 3382-3 [2] and NS 8175 [6].

Two simulation model with Odeon were used. They were chosen to evaluate the impact of allowing different absorption and scattering coefficients in the two Zones. Points of improvement would be to estimate the simulations using a more realistic source than a point source. Another improvement proposal is fine tuning of the input parameters. It would have been interesting to do the same simulations using CATT, and compare those results with the results from Odeon. The results show that the reverberation time in simulation model 2 is closer to the measured RT in Zone 2. Both for the A-weighted SPL based parameters and the STI based parameters, the values from simulation model 1 are closer to the measured values. For the A-weighted SPL based parameters, both simulation models give much lower values than for the measurements, except at Zone 1 ML2. For the STI based parameters, the simulation models are somewhat in the same area as the measured results for Zone 1. However, in Zone 2, the simulated r_p is much longer than the measured, this is due to the unsteady decline of the STI versus S-R distance.

It was expected that the simulations should attenuate the sound more than the measurements, since the transparency factor was set to zero. In a real situation, some sound will pass through materials or set materials in motion such that sound is mirrored to the other side.

An important lesson learned through this thesis work is that doing acoustic measurements and simulations requires skill and experience, which I hope to further develop in my professional career.

Bibliography

[1] ISO 3382-1. *Acoustics - Measurements of roomacoustic paramters Part1: Rooms for presentation*. International Organization for Standardization, 2009.

[2] ISO 3382-3. *Acoustics - Measurements of roomacoustic paramters Part3: Open-plan offices*. International Organization for Standardization, 2012.

[3] ANSI S 3.5-1997. *Methods for the calculation of the speech intelligibility index.* American National Standard Institute, R 2007.

[4] NEK EN 60268-16. *Sound system equipment Part 16: Objective rating of speech intelligibility by speech transmission index*. International Electrotechnical Commission (IEC), 2003.

[5] NEK EN 60268-16. *Sound system equipment Part 16: Objective rating of speech intelligibility by speech transmission index*. International Electrotechnical Commission (IEC), 2011.

[6] NS 8175. *Acoustical conditions in buildings Sound classification of various types of buildings*. Standards Norway, 2012.

[7] J. S. Bradley. *The acoustical design of conventional open plan office*. Institute for Research in Construction, National Research Council, Montreal Rd. Ottawa, Kl A 0R6, 2003.

[8] Hilge C. and Noche C. *Office acoustics*. Buero-forum, 2001.

[9] C. L. Christensen and G. Koutsouris. *Odeon User Manual, Version 12*. Odeon A/S, Diplomvej, building 381, DK-2800 Kgs. Lyngby, Denmark, 2 edition, 01 2013.

[10] The Physics Classroom. Reflection, Refraction, and Diffraction. `http://www.physicsclassroom.com/class/waves/Lesson-3/Reflection,-Refraction,-and-Diffraction`. Accessed: 2017-02-20.

[11] Bengt-Inge Dalenbeck. Private communication, email. 2017-02-15.

[12] Christina B. Danielsson. *Office Environment, Health and Job Satisfaction, Licentiate Thesis*. Stockholm, Sweden, KTH Technology and Health., 2005.

[13] Jacob Donley. The Speech Transmission Index (STI). `https://se.mathworks.com/matlabcentral/fileexchange/62512-the-speech-transmission-index--sti-`. Accessed: 2017-05-29.

[14] W. Ellermeier and J. Hellbrck. *Is level irrelevant in irrelevant speech? Effects of loudness, signal-to-noise ratio, and binaural unmasking, Journal of Experimental Psychology: Human Perception and Performance*. Ergonomics, 1998. 1406-1414.

[15] A. Haapakangas, R. Helenius, E. Keskinen, and V. Hongisto. *Perceived acoustic environment, work performance and well-being survey results from Finnish offices*. Griefahn, B. (ed.) Proceedings of ICBEN 2008, Connecticut, USA, Mashantucket, The 9th Congress of the International Commission on the Biological Effects of Noise., 2008. 434-441.

[16] M. Haka, A. Haapakangas, J. Kernen, J. Hakala, E. Keskinen, and V. Hongisto. *Performance effects and subjective disturbance of speech in acoustically different office types a laboratory experiment*. Indoor Air, 2009. 454-467.

[17] Daniela T. Helboe. Private communication, email. 2017-06-13.

[18] Valtteri Hongisto. *A model predicting the effect of speech of varying intelligibility on work performance*. Indoor Air, 2005. 458-468.

[19] Valtteri Hongisto. *WORK PERFORMANCE AND OFFICE NOISE - DO THEY CORRELATE?* Finnish Institute of Occupational Health, Indoor Environment Laboratory, 20520 Turku, Finland, 2007.

[20] A. Kaarlela-Tuomaala, R. Helenius, V. Hongisto, and E. Keskinen. *Does office noise disturb work performance more in open-plan than in single room offices? a case study*. XXVIII International Congress of Psychology, (abstract), Beijing, China, 2004.

[21] MathWorks. Octave-Band and Fractional Octave-Band Filters. `https://se.mathworks.com/help/audio/examples/octave-band-and-fractional-octave-band-filters.html`. Accessed: 2017-05-15.

[22] L. H. Morset, A. Goldberg, P. Svensson, and J. R. Mathiassen. *WinMLS 2000 User's Guide, Version 3.00*. Morset Sound Development, Persauneveien 25, 7045 Trondheim, Norway, 1 edition, 11 2001.

[23] Norsonic. Helkule hyttaler Nor276. `http://no.norsonic.com/product/helkule-hoyttaler-nor276/`. Accessed: 2017-05-31.

[24] Allan D. Pierce. *Diffraction of sound around corners and over wide barriers*. The Journal of the Acoustical Society of America, 1974.

[25] J. H. Rindel, G. B. Nielsen, and C. L. Christensen. *Diffraction around corners and over wide barriers in room acoustic simulations*. Odeon A/S, Scion DTU, Denmark, 2009.

[26] Peter Svensson. Private communication, email. 2017-02-28.

[27] Peter Svensson. Software and measurement data for download; edge diffraction toolbox. `http://www.iet.ntnu.no/~svensson/software/index.html`. Accessed: 2017-02-03.

[28] N. Venetjoki, A. Kaarlela-Tuomaala, E. Keskinen, and V. Hongisto. *The effect of speech and speech intelligibility on task performance*. Ergonomics, 2006. 10681091.

[29] P. Virjonen, J. Keranen, and V. Hongisto. *Determination of acoustical conditions in open-plan offices: proposal for new measurement method and target values*. Acta Acustica united with Acustica, 2009.

[30] R. E. Walpole, R. H. Mayers, S. L Mayers, and K. Ye. *Probability & Statistics for Engineers & Scientitsts, 9. edition*. Pearson Education, Inc, 2012.

Appendix

A Matlab codes

A.1 STI function

The function was altered for estimating the Odeon results, but the same logic was used. The find level difference part was a scale factor. The function is based on Jacob Donely's STI function [13].

```
function[STI_val] = STI_mod(filename, bgn, Lps_1m)

%% Load IR's
[IR_ref, Fs] = loadimp('Ref_1m_1_.wmb');
[IR] = loadimp(filename);

%% Level difference for the scaled ".wmb"
Level_diff = 151.4395;

%% Rectangular filter of reference, to remove reflections.
IR_ref(350:end) = 0;

%% Octaveband filtering
[filteredIR, F0] = OctaveFilter(IR, Fs);
FR = 10*log10(sum((filteredIR).^2))';

[filteredIR_ref, F0] = OctaveFilter(IR_ref, Fs);
FR_ref_oct = 10*log10(sum(filteredIR_ref.^2))';

%% Creat white noise
Noise = wgn(105600,1,26);
[filteredNoise, F0] = OctaveFilter(Noise, Fs);

%% Find (S/N)
D = FR_ref_oct(3:end-1) - FR(3:end-1);
LpSni = Lps_1m - D';
SNR = LpSni-bgn;

%% Synthesise IR with noise using (S/N) and wgn
```

```
E_sig = sum(filteredIR.^2);
E_sig = E_sig(3:end-1);

E_noise = sum(filteredNoise.^2);
E_noise = E_noise(3:end-1);

for i = 1:7
    scale(i) = E_sig(i)/((10^(SNR(i)/10))*E_noise(i));
end

IRmstoy_squared = zeros(105600,7);
for i = 1:7
    IRmstoy_squared(:,i) = (filteredIR(:,i+2).^2) + ...
    (scale(i)*(filteredNoise(:,i+2)).^2);
end

%% Estimate MTF
nfft = length(IR);

for i =1:7
    MTF_octband(:,i) =  ...
    abs(fft(IRmstoy_squared(:,i),nfft)/sum(IRmstoy_squared(:,i)));
end
% Only keep bands in the range required for the STI calculation
F0(F0<125 | F0>min([8000,Fs/2]))=[];
Nfc = length(F0);

modulation_freqs = 2 .^ ([-2:11]./3);
%No nyquist frequency
freqs = linspace(0, Fs/2, size(MTF_octband,1)/2+1); freqs(end)=[];

for i=1:Nfc
        m(i,:) = interp1(freqs,MTF_octband(1:end/2,i),modulation_freqs);
end
good_freqs = ~any(isnan(m),2);
m(~good_freqs,:)=[];

%% Convert each of the 98 m values into an
%% apparent signal-to-noise ratio (S/N) in dB
SNR_apparent = pow2db( m ./ (1-m) );

%% Limit the Range
SNR_apparent( SNR_apparent > 15 ) = 15;
SNR_apparent( SNR_apparent < -15 ) = -15;

```

```
%% Compute the mean (S/N) for each octave band
SNR_avg = mean(SNR_apparent,2);

%% Weight the octave mean (S/N) values
% Values from the STI standard
W = [0.13, 0.14, 0.11, 0.12, 0.19, 0.17, 0.14];
SNR_Wavg = sum(SNR_avg' .* W(good_freqs));
SNR_Wavg_approx = sum(SNR_avg' .* W(good_freqs)/sum(W(good_freqs)));

%% Convert the overall mean (S/N) to an STI value
STI_val = (SNR_Wavg + 15) / 30;
STI_val_approx = (SNR_Wavg_approx + 15) / 30;
```

A.2 Distance attenuation function

The function estimates $L_{p,A,S,n}$ and $D_{2,S}$ according to Equations 3.3 and 3.4, respectively. The function was altered for estimating the Odeon results, but the same logic was used. The find level difference part was a scale factor.

```
function [D2S, L_pAS_n] = DistAttenu(Filenames, r)

%%%%%%%%%%%%%%%%%%%%%%%%%%%%%%%%%%%%%%%%%%%%%%%%%%%%%%%%%%%%%%%%%%%%
%% Find the level difference between matlab and WinMLS
[ref, Fs] = loadimp('Ref_1m_1_.wmb');
tempref1m = OctaveFilter(ref, Fs);
refsig1m_oct = 10*log10(mean(tempref1m.^2))';
G = [63.2 71.1 67.5 65.3 66.8 77.7 68.9]; % From WinMLS
Level_diff = G - refsig1m_oct(3:end-1)';
Level_diff = Level_diff(3);
%%%%%%%%%%%%%%%%%%%%%%%%%%%%%%%%%%%%%%%%%%%%%%%%%%%%%%%%%%%%%%%%%%%%

y = length(Filenames);
for i = 1:y
    [IR_L1(:,i)] = loadimp(char(Filenames(i)));
end

%% Truncate the impulse respone of the reference
% rectangular window
IR_ref = ref;
IR_ref(350:end) = 1*10^(-18);

%% Oktaveband filtering

for i = 1:y
[filteredIR_L1, F0] = OctaveFilter(IR_L1(:,i), Fs);
Level(:,i) = 10*log10(mean(filteredIR_L1.^2))';
```

```
end

[filteredIR_ref, F0] = OctaveFilter(IR_ref, Fs);
FR_ref_oct = 10*log10(mean(filteredIR_ref.^2))';

oct = [125 250 500 1000 2000 4000 8000];

FR_refe = FR_ref_oct(3:end-1)+ Level_diff;
FR_meas = Level(3:end-1,i)+ Level_diff;

%% Delta
D_n_i = zeros(y,7);
for i = 1:y
    D_n_i(i,:) = FR_ref_oct(3:end-1) - Level(3:end-1,i);
end

%% L_pAS_n
Lps_1m = [49.9 54.3 58.0 52.0 44.8 38.8 33.5];
Aw =[-16.1 -8.6 -3.2        0 1.2 1        -1.1];
%L_pS_ni(i,:) = zeros(4:7);
temp = zeros(4,7);
for i = 1:y
    L_pS_ni(i,:) = Lps_1m - D_n_i(i,:);
    temp(i,:) = 10.^((L_pS_ni(i,:)+Aw)./10);
end

L_pAS_n = 10*log10(sum(temp'));

%% D2S
N = y; % # Meas. pos.
r0 = 1; %Ref. dist.
r = r; % Meas. dist.
over = N*sum(L_pAS_n.*log10(r./r0)) - sum(L_pAS_n)*sum(log10(r./r0));
under = N*sum((log10(r./r0)).^2) - (sum(log10(r./r0))).^2;

D2S = -log10(2)*(over/under);
```

A.3 Octave band filter function

The function filters an IR into octave bands, it is based on MathWorks [21]. A similar function can also be found in Jacob Donely's STI function [13].

```
function [filteredIR, F0] = OctaveFilter(Impulse, Fs)

 % Filter spesifikasjon
 BandsPerOctave = 1; % number of bands per octave
```

```
N = 6; % Filterorder
F0 = 1000; % Center frequency

%%
f = fdesign.octave(BandsPerOctave,'Class 1','N,F0',N,F0,Fs); % Spec
F0 = f.validfrequencies; % Frequency bands
Nfc = length(F0);
for j = 1:Nfc,
f.F0 = F0(j);
Hd(j) = design(f,'butter');
end

for j = 1:length(F0)
filteredIR(:,j) = filter(Hd(j),Impulse);
end

end
```

B Diffraction analysis

B.1 1. and 2. order diffraction results with Odeon, CATT and EDB, using S_1 and thick screen.

S_1 and receiver positions 5, 10 and 13-20.

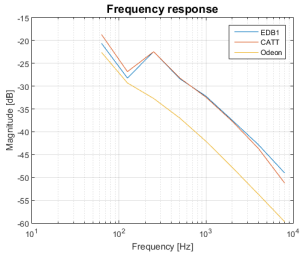

(a) FR, S_1 and R_5

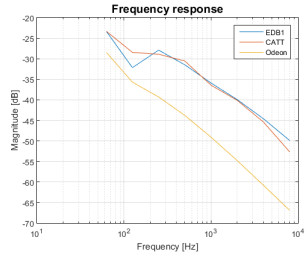

(b) FR, S_1 and R_{10}.

Figure 1: Odeon, CATT and EDB1, FR thick screen, S_1 and R_5 and R_{10}.

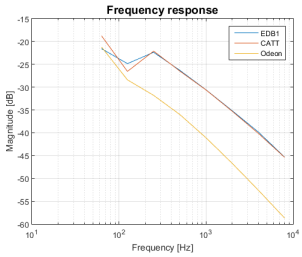

(a) FR, S_1 and R_{13}.

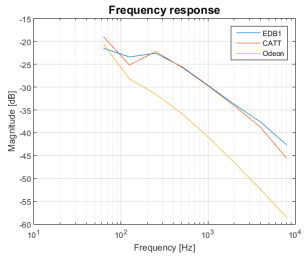

(b) FR, S_1 and R_{14}.

Figure 2: Odeon, CATT and EDB1, FR thick screen, S_1 and R_{13} and R_{14}.

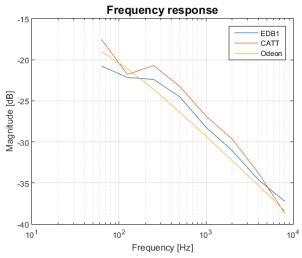

(a) FR, S_1 and R_{15}..

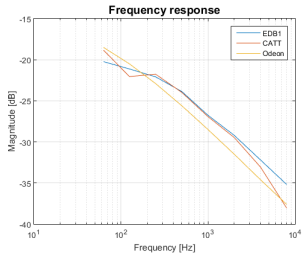

(b) FR, S_1 and R_{16}.

Figure 3: Odeon, CATT and EDB1, FR thick screen, S_1 and R_{15} and R_{16}.

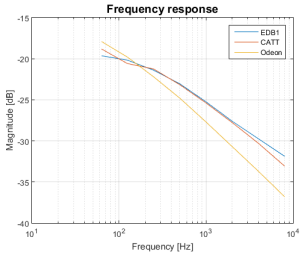

(a) FR, S_1 and R_{17}.

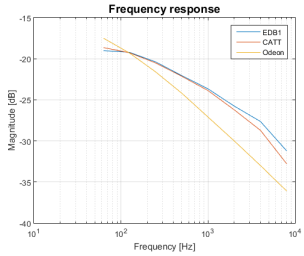

(b) FR, S_1 and R_{18}.

Figure 4: Odeon, CATT and EDB1, FR thick screen, S_1 and R_{17} and R_{18}.

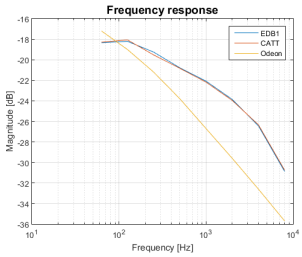

(a) FR, S_1 and R_{19}.

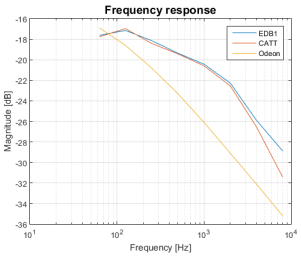

(b) FR, S_1 and R_{20}.

Figure 5: Odeon, CATT and EDB1, FR thick screen, S_1 and R_{19} and R_{20}.

B.2 1. and 2. order diffraction results with Odeon, CATT and EDB, using S_2 and thick screen.

S_2 and receiver positions 1, 5, 7, 10 and 13-18.

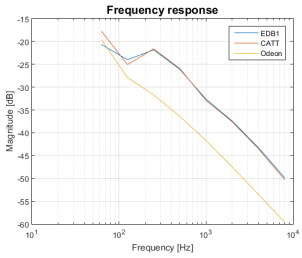

(a) FR, S_2 and R_1

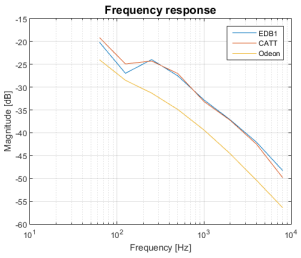

(b) FR, S_2 and R_5

Figure 6: Odeon, CATT and EDB1, FR thick screen, S_2 and R_1 and R_5.

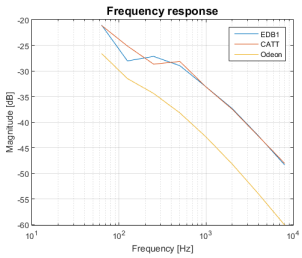

(a) FR, S_2 and R_7

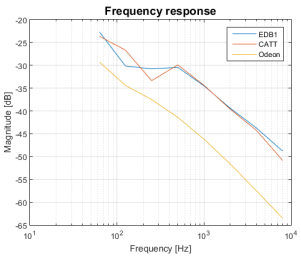

(b) FR, S_2 and R_{10}

Figure 7: Odeon, CATT and EDB1, FR thick screen, S_2 and R_7 and R_{10}.

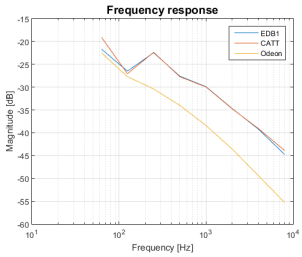

(a) FR, S_2 and R_{13}

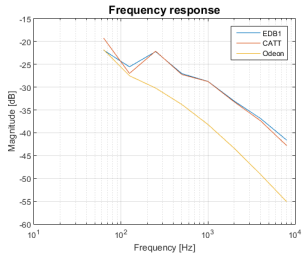

(b) FR, S_2 and R_{14}

Figure 8: Odeon, CATT and EDB1, FR thick screen, S_2 and R_{13} and R_{14}.

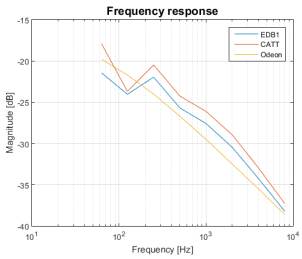

(a) FR, S_2 and R_{15}

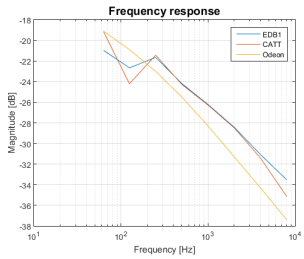

(b) FR, S_2 and R_{16}

Figure 9: Odeon, CATT and EDB1, FR thick screen, S_2 and R_{15} and R_{16}.

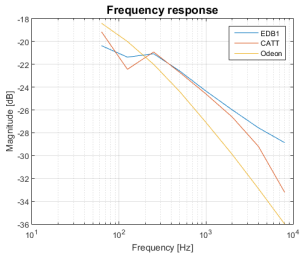

(a) FR, S_2 and R_{17}

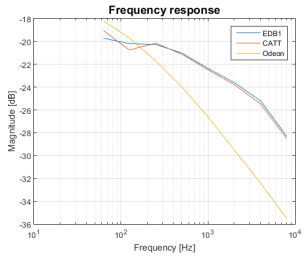

(b) FR, S_2 and R_{18}

Figure 10: Odeon, CATT and EDB1, FR thick screen, S_2 and R_{17} and R_{18}.

C Measured and simulated RT

The RT at each position along ML1 in Zone 1 and 2, from measurements, simulation model 1 and simulation model 2.

C.1 RT measured

Table 1: Measured RT in Zone 1 and 2 along ML 1.

	Freq [Hz]	125	250	500	1000	2000	4000	8000
	Zone 1 ML 1							
RT in pos #	**Pos 1**	0.40	0.33	0.28	0.27	0.32	0.36	0.35
	Pos 2	0.38	0.35	0.31	0.33	0.41	0.44	0.43
	Pos 3	0.40	0.37	0.34	0.33	0.39	0.42	0.40
	Pos 4	0.47	0.36	0.31	0.35	0.39	0.33	0.33
	Zone 2 ML 1							
RT in pos #	**Pos 1**	0.37	0.29	0.25	0.29	0.32	0.33	0.35
	Pos 2	0.34	0.29	0.27	0.29	0.33	0.35	0.34
	Pos 3	0.38	0.30	0.29	0.29	0.35	0.39	0.38
	Pos 4	0.39	0.33	0.29	0.30	0.36	0.40	0.39
	Pos 5	0.41	0.32	0.32	0.33	0.42	0.40	0.39

C.2 RT simulation model 1

Table 2: Simulation model 1, RT in Zone 1 and 2 along ML 1.

	Freq [Hz]	125	250	500	1000	2000	4000	8000
	Zone 1 ML 1							
RT in pos #	**Pos 1**	0.39	0.32	0.29	0.29	0.35	0.35	0.27
	Pos 2	0.41	0.34	0.30	0.31	0.39	0.40	0.29
	Pos 3	0.41	0.34	0.31	0.30	0.32	0.33	0.27
	Pos 4	0.41	0.34	0.31	0.32	0.33	0.33	0.30
	Zone 2 ML 1							
RT in pos #	**Pos 1**	0.38	0.36	0.40	0.42	0.43	0.44	0.38
	Pos 2	0.39	0.33	0.33	0.37	0.40	0.40	0.35
	Pos 3	0.39	0.37	0.40	0.38	0.39	0.40	0.34
	Pos 4	0.38	0.33	0.32	0.35	0.37	0.38	0.33
	Pos 5	0.38	0.34	0.36	0.38	0.39	0.40	0.36

C.3 RT simulation model 2

Table 3: Simulation model 2, RT in Zone 1 and 2 along ML 1.

	Freq [Hz]	**125**	**250**	**500**	**1000**	**2000**	**4000**	**8000**
	Zone 1 ML 1							
RT in pos #	**Pos 1**	0.38	0.34	0.30	0.31	0.32	0.32	0.29
	Pos 2	0.40	0.34	0.30	0.30	0.30	0.31	0.28
	Pos 3	0.40	0.34	0.31	0.32	0.33	0.35	0.29
	Pos 4	0.40	0.34	0.31	0.31	0.33	0.49	0.29
	Zone 2 ML 1							
RT in pos #	**Pos 1**	0.37	0.30	0.30	0.32	0.34	0.36	0.32
	Pos 2	0.38	0.30	0.31	0.33	0.36	0.46	0.30
	Pos 3	0.38	0.29	0.27	0.30	0.31	0.32	0.27
	Pos 4	0.38	0.30	0.28	0.28	0.29	0.30	0.26
	Pos 5	0.37	0.26	0.23	0.25	0.25	0.25	0.23

D Material properties

D.1 Tropic

TROPIC

TROPIC

· Tropic kombinerer en matt, hvit overflate med de beste egenskaper med hensyn til akustikk, brannsikkerhet og fuktmotstand

· Med Tropic-sortimentet er det mulig å skape himlingseffekter med både delvis skjulte profiler (E-kant) og fullt synlige profiler (A-kant)

PRODUKTBESKRIVELSE

· Plate i steinull
· Forside: Matt, hvit overflate
· Bakside: Baksidefleece
· Malte kanter

SORTIMENT

Kant	Modulmål (mm)	Vekt pr. m^2	MKH*) / MKH*) for demontasje (mm)	Montasjesystem
A24 	600 x 600 x 15 1200 x 600 x 15 600 x 600 x 40 1200 x 600 x 40	1,9 1,9 3,5 3,5	50 / 100 50 / 100 40 / 200 40 / 200	Rockfon System T24 A/E Rockfon System XL T24 A/E
E15 	600 x 600 x 15	2,1	58/100	Rockfon System T15 A/E
E24 	600 x 600 x 15 1200 x 600 x 15	2,1 2,1	58 / 100 58 / 100	Rockfon System T24 A/E Rockfon System XL T24 A/E

**) MKH = Minste konstruksjonshøyde*

EGENSKAPER

Lydabsorpsjon

α_w = opptil 0,95 (Klasse A)

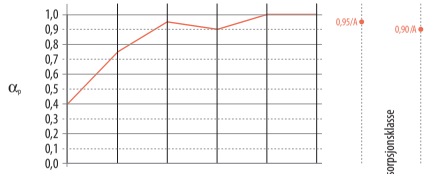

Tykkelse (mm) / konstruksjonshøyde (mm)	125 Hz	250 Hz	500 Hz	1000 Hz	2000 Hz	4000 Hz	α_w	Absorpsjonsklasse	NRC
15 / 200*	0,40	0,75	0,95	0,90	1,00	1,00	0,95	A	0,90

** Der er ikke foretatt måling for Tropic 40 mm. Verdiene i lydkurven gjelder for Tropic 15 mm plater.*

Brannklasse
A1

Lysrefleksjon
86%

Fuktmotstand og formstabilitet
Opptil 100% RH
1/C/0N

Rengjøring
Støvsuging

Hygiene
Steinull danner ingen grobunn for mikroorganismer

Miljø
100 % resirkulerbart

Inneklima
En utvalg av ROCKFONs produkter er blitt tildelt

D.2 Krios

KRIOS dB 42

ROCKWOOL Rockfon®

CREATE AND PROTECT®

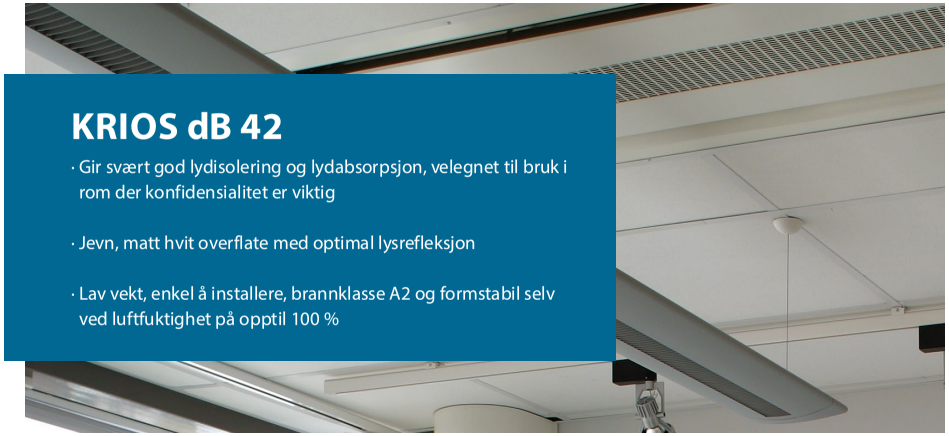

KRIOS dB 42

· Gir svært god lydisolering og lydabsorpsjon, velegnet til bruk i rom der konfidensialitet er viktig

· Jevn, matt hvit overflate med optimal lysrefleksjon

· Lav vekt, enkel å installere, brannklasse A2 og formstabil selv ved luftfuktighet på opptil 100 %

PRODUKTBESKRIVELSE

· Plate i steinull
· Forside: Jevn, matt overflate
· Bakside: Høykvalitets membran
· Malte kanter

SORTIMENT

Kant	Modulmål (mm)	Vekt pr. m²	MKH*) / MKH*) for demontasje (mm)	Montasjesystem
A24	600 x 600 x 40 1200 x 600 x 40	7,1 7,1	50 / 200 50 / 200	Rockfon System T24 A/E
D	600 x 600 x 40	7,1	-	Rockfon System XLT24 D
D/A EX	600 x 600 x 40 1200 x 600 x 40	7,1 7,1	60 / 200 60 / 200	Rockfon System Bandraster D/A
E15	600 x 600 x 40 1200 x 600 x 40	7,1 7,1	60 / 200 60 / 200	Rockfon System T15 A/E
E24	600 x 600 x 40 1200 x 600 x 40	7,1 7,1	60 / 200 60 / 200	Rockfon System T24 A/E

*) MKH = Minste konstruksjonshøyde

EGENSKAPER

Lydabsorpsjon

α_w = opptil 0,90 (Klasse A)

Rom-til-rom-lydisolering

$D_{n,f,w}$ ($C;C_{tr}$) = 42 (-2;-7) dB

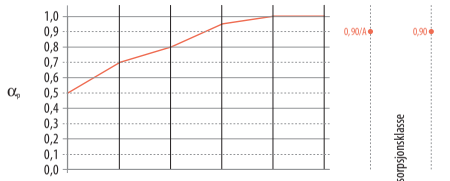

Tykkelse (mm) / konstruksjonshøyde (mm)	125 Hz	250 Hz	500 Hz	1000 Hz	2000 Hz	4000 Hz	α_w	Absorpsjonsklasse	NRC
40 / 200	0,50	0,70	0,80	0,95	1,00	1,00	0,90	A	0,90

Brannklasse

A2-s1,d0

Lysrefleksjon

86%

Fuktmotstand og formstabilitet

Opptil 100% RH

Rengjøring

Støvsuging

Hygiene

Steinull danner ingen grobunn for mikroorganismer

Miljø

100 % resirkulerbart

Inneklima

En utvalg av ROCKFONs produkter er blitt tildelt

THE INDOOR CLIMATE LABEL M1 EMISSION CLASS FOR BUILDING MATERIAL

Varmeledningsevne

λ_D = 40 mW/mK

D.3 Suspended ceiling

A-KANT PÅ ALL HIMLING I 4.ETASJE.

5. og 6. etasje er lik som 4. etasje.

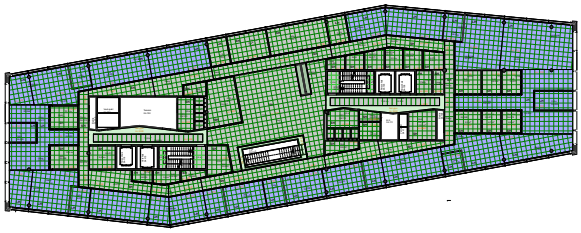

Standard Himling

Lyd Himling

N

J	fast gips over kjøkken/ garderobe, m/ skjørt i overgang fast gips/ syn. himling	AJT	ES		22.04.15
I	Tatt ut skjørt der gips og syn.himling i samme høyde.	AJT	ES		18.03.15
H	Oppdatert utsendelse iht. kom. fra AF	AJT	ES		10.03.15
Rev.	Revideringen gjelder	Tegn.	Kont.	Godkj.	Dato

A	ARK	LØF ARKITEKTER AS	Telefon: 22 98 97 70
B	RIB		Saks nr.: 2529 Cowi (1807)
Vv	RIVV		Telefon:
Vr	RIV		Saks nr.:
E	El.tek		Telefon:
			Saks nr.:
			Telefon:
			Saks nr.:

Prosjekt: HasleLinje AS Bygg K2A | Adresse: | Kvartalsnr. (ARK): 1807 | Tegn: KN | Kontr: ES | Godkj:

Dato: 24.09.14

Type tegning: Himlingsplan 4.etg.

Ark: A1 | Målestokk: 1:100

Filnavn: K2A_Hovedmodell_2

Lok: K2A | Tegn. nr.: A_P_25_04 | Rev: J

Hasle Linje AS
C/o Hiegh Eiendom AS
Postboks 2416 Solli - 0201 Oslo

D.4 Epoca Structure

Epoca Structure

Produktbeskrivelse

ege
design · quality · respect

Produktbeskrivelse	Metoder	Produktdata
Konstruktion		
Struktur	ISO 2424	Vævet loop pile
Luvmateriale	DIR 96/73, 96/74	100% Polyamid
Farvemetode	-	Continue
Bagside	eTL	WT - Vævet tekstil
Dimensioner	ISO 3018	400 cm
Totalhøjde		Ca. 0,18""
	ISO 1765	Ca. 4,5 mm.
Totalvægt	ISO 8543	Ca. 2.300 g/m2
Luvindsatsvægt	eTL	700 g/m2
ege soil protection	eTL	Ja
Egnethedsprøvninger		
Brugsområder	EN15114	33 Erhverv - Kraftig brug
Garanti mod gennemslid	eTL	Contract certifikat
Brugsområder	Gulvbranchen	Klasse 33
Rullehjulsegnet	EN 985	Ja, konstant brug
Trappeegnet	EN 1963	Ja
Antistatiske egenskaber	eTL	Permanent antistatisk
Personopladning	ISO 6356	Antistatisk
Trinlydsdæmpning	eTL	16 dB
Akustisk absorption	eTL	0,15 aW
Gulvvarmeegnet	ISO 8302	Ja
Lysægthed	ISO 105-B02	>5
	AATCC 16	5.0
Gnideægthed våd	EN ISO 105-X12	>3
	AATCC 165	5.0
Gnideægthed tør	EN ISO 105-X12	>3-4
	AATCC 165	5.0
Vandægthed mønstrede/melerede	EN ISO 105-E01	>4
Cleaning	AATCC 138	5.0
Colour fastness to Ozone	AATCC 129	4.5
Colour fast.Oxides of Nitrogen	AATCC 164	4.5
Øvrige brugstests	ASTM D5252 Hexapod	4.5/ 4.5
Sikkerhed & Miljø		
CE Mærkning	EN 14041	Certificeret
EC Certifikat	EN 14041	2531-CPR-CXA10010C
CE Mærkning	Ydeevnedeklaration	DOP 9711-10C
Brandklassifikation	DK,MK GODKENDELSE	Godkendt
	D,DIBT AbZ.no.	Z-156.601-377
	CH,VKF/AEAI	Cfl-s1
	ASTM E-648	Class 1
	ASTM E662 Smoke Density	<450
	ASTM D2859 Surface Flamm.	Pass
	EN13501-1 euro class	Cfl-s1

ege
design · quality · respect

Produktbeskrivelse	Metoder	Produktdata
	AU,ASISO 9239.1-2003	4,70 KW/m2
Indeklima	DIM Certifikat	No.006
	LEED	Green Label Plus Test
	Emissions dans l'air intérieur	A+/A+
	GECA	Godkendt
Miljø	Byggvarudeklaration	BVD 3
	Environmental Product Decl.	EPD-EGE-20130067-CBD1-EN
Vejledninger		
Montering, inkl. limguide	DK	Dansk
	N	Norsk
	S	Svensk
	GB	English
	D	Deutsch
	F	Francais
Rengøring, pletfjerning	DK	Dansk
	N	Norsk
	S	Svensk
	GB	English
	D	Deutsch
	F	Francais
Producent		
Fabrikscertificering	ISO 9001	Audited and verified by BVC
	ISO 14001	Audited and verified by BVC
	EMAS	Audited and verified by BVC
	OHSAS	Audited and verified by BVC
	DS 49001	Audited and verified by BVC
	CRuk	Member of Carpet Recycling UK
	TransQ	Qualified

D.5 Screens

I. Skjerm-elementer

Nr	Materialtype	Overflate	Tett kjerne mm	Absorbent én/to-sidig	Total tykkelse mm
1	Becker-Akustik Bullermodul	Netting	0,9, stål	én	40
2	Butikkmontering A/S	Plaststrie	3,5, trefiber	to	44
3	Grünzweig & Hartmann	Strekkmetall	Skumkjerne	to	—
4	Gullfiber støymodul	Stålplate	Stål	én	40
4	Gullfiber støymodul	Stålplate	Stål	to	70
5	Gullfiber system RG	Stålplate	Stål	én	70
6	Hedmora type EP	Stålplate	Stål	én	80
7	Hov Møbelindustri Modul 40	Tekstil	3,5, trefiber	to	29
8	Nobø systemvegg	Tekstil	0,55, stål	to	80
9	Perfoverken AB Perfovegg	Stålplate	1,0, stål	én	50
9	Perfoverken AB Perfovegg	Stålplate	1,0, stål	to	50
10	Perfoverken AB Perfovegg	Stålplate	1,0, stål	én	100
10	Perfoverken AB Perfovegg	Stålplate	1,0, stål	to	100
11	Verkstads AB Q-industrisystem	Stålplate	1,0, stål	én	42
11	Verkstads AB Q-industrisystem	Stålplate	1,0, stål	to	42
12	Rockwool Rockfon Veggelement	Stålplate	0,7, stål	én	50
12	Rockwool Rockfon Veggelement	Stålplate	0,7, stål	én	50
12	Rockwool Rockfon Takelement	Mineralull	0,7, stål	to	200
13	Skjermvegg (spesialvegg, NRK)	Trefiber	0,7, stål	to	34
14	Skjermvegg fra Stål & Stil A/S	Tekstil	10, spon	to	35

AKUSTISK LABORATORIUM
TILSLUTTET SINTEF
NORGES TEKNISKE HØGSKOLE
TRONDHEIM

ABSORPSJONSFAKTORER målt i klangrom
(ISO R354)

Hz	α
63	
80	
100	.17
125	.18
160	.22
200	.30
250	.50
315	.70
400	.90
500	.97
630	1.00
800	1.00
1000	1.00
1250	1.00
1600	1.00
2000	1.00
2500	1.00
3150	1.00
4000	1.00
5000	1.00
6300	

MATERIALE : Type I1

Skjerm-moduler
type Becker-Akustikk Buller-moduler

α absorpsjonsfaktor

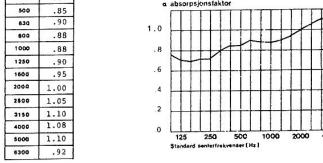

MÅLEBESKRIVELSE :

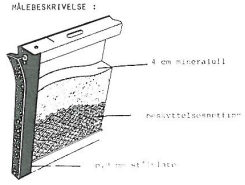

Modulstørrelse fra
30 x 30 cm^2 opp til
60 x 2400 cm^2 i stepp på
30 cm.

I 1

AKUSTISK LABORATORIUM
TILSLUTTET SINTEF
NORGES TEKNISKE HØGSKOLE
TRONDHEIM

ABSORPSJONSFAKTORER målt i klangrom
(ISO R354)

Hz	α
63	
80	
100	.76
125	.72
160	.70
200	.72
250	.72
315	.80
400	.85
500	.85
630	.90
800	.88
1000	.88
1250	.90
1600	.95
2000	1.00
2500	1.05
3150	1.10
4000	1.08
5000	1.10
6300	.92

MATERIALE : Type I3

Skjermvegg
fra Grünzweig & Hartmann
und Glasfaser AG.

α absorpsjonsfaktor

MÅLEBESKRIVELSE :

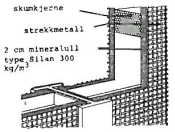

I 3

AKUSTISK LABORATORIUM
TILSLUTTET SINTEF
NORGES TEKNISKE HØGSKOLE
TRONDHEIM

ABSORPSJONSFAKTORER målt i klangrom
(ISO R354)

Hz	A
63	
80	
100	.20
125	.31
160	.37
200	.40
250	.45
315	.48
400	.63
500	.90
630	1.34
800	1.79
1000	1.87
1250	1.50
1600	1.13
2000	.95
2500	.85
3150	.79
4000	.70
5000	
6300	

MATERIALE : Type I2

Skjermvegg fra A/S Butikkmontering.

A, ekvivalent absorpsjonsareale, m^2 Sabin/m^2 skjerm

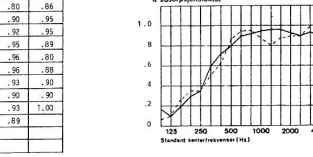

MÅLEBESKRIVELSE :

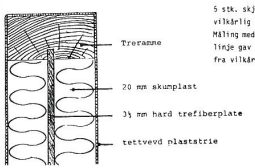

5 stk. skjermer á 855 mm x 1470 mm vilkårlig fordelt på gulvflaten. Måling med skjermer oppstilt på én linje gav ingen signifikante avvik fra vilkårlig fordeling.

I 2

AKUSTISK LABORATORIUM
TILSLUTTET SINTEF
NORGES TEKNISKE HØGSKOLE
TRONDHEIM

ABSORPSJONSFAKTORER målt i klangrom
(ISO R354)

Hz	α_1	α_2
63		
80		
100	.16	.06
125	.10	.10
160	.19	.26
200	.30	.35
250	.35	.35
315	.60	.50
400	.72	.63
500	.80	.86
630	.90	.95
800	.92	.95
1000	.95	.89
1250	.96	.80
1600	.96	.88
2000	.93	.90
2500	.90	.90
3150	.93	1.00
4000	.89	
5000		
6300		

MATERIALE : Type I4

Perforert stålpanel type Gullfiber
Støymodul

α absorpsjonsfaktor

MÅLEBESKRIVELSE :

Produkt: Stålplatevegg, 40 eller 70 mm tykk, 2000 x 500 mm^2 eller 2000 x 1000 mm^2.
En eller begge sider perforert med 24 mm hull, innlegg av Gullfiber mineralullmatte.

——— = En side perforert, 40 mm tykk vegg

------- = Begge sider perforert, 70 mm tykk vegg

Støymodulene målt fritt plassert på gulv

Bruksområde: Støyavskjerming. Kan også leveres montert på en tralle: Gullfiber MOBIDUL. Modul er da 30 mm tykk, modulbredde 1000 mm.

I 4

AKUSTISK LABORATORIUM
TILSLUTTET SINTEF
NORGES TEKNISKE HØGSKOLE
TRONDHEIM

ABSORPSJONSFAKTORER målt i klangrom
(ISO R354)

Hz	α
63	
80	
100	.05
125	.10
160	.25
200	.34
250	.34
315	.50
400	.65
500	.85
630	.95
800	.94
1000	.90
1250	.82
1600	.90
2000	.90
2500	.92
3150	1.00
4000	
5000	
6300	

MATERIALE : Type I5

Skjermvegg type Gullfiber system RG.

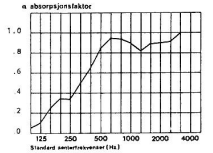

MÅLEBESKRIVELSE :

Skjermvegg: 70 mm tykke metall-veggelementer, standard høyde 2500 og 3000 mm, bredde 1000 mm og 500 mm. Takelementer, veggelementer med dør og vindu leveres for innebygging av støykilder e.l. Elementene leveres perforert på én eller begge sider med 70 mm mineralullmatte mellom metallplatene.

——— = Målt veggelement med en side perforert, element fritt plassert på gulv.

I 5

AKUSTISK LABORATORIUM
TILSLUTTET SINTEF
NORGES TEKNISKE HØGSKOLE
TRONDHEIM

ABSORPSJONSFAKTORER målt i klangrom
(ISO R354)

Hz	A
63	
80	
100	.19
125	.25
160	.19
200	.24
250	.26
315	.34
400	.37
500	.35
630	.46
800	.50
1000	.58
1250	.65
1600	.77
2000	.77
2500	.89
3150	.97
4000	.97
5000	
6300	

MATERIALE : Type I7

Kontorskjermvegg fra Hov Møbelindustri, Modul 40

A, ekvivalent absorpsjonsareale, m^2 Sabin/m^2 skjerm

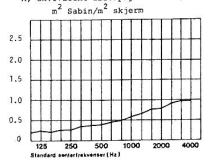

MÅLEBESKRIVELSE :

6 stk. vegger á 780 mm x 1510 mm vilkårlig oppstilt på gulv i klangrom.

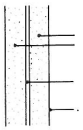

12½ mm nordø trefibermlate

3½ mm hard trefiberplate

tekstilkledning

I 7

AKUSTISK LABORATORIUM
TILSLUTTET SINTEF
NORGES TEKNISKE HØGSKOLE
TRONDHEIM

ABSORPSJONSFAKTORER målt i klangrom
(ISO R354)

Hz	α
63	
80	
100	.22
125	.26
160	.78
200	.76
250	.80
315	.71
400	.88
500	.81
630	.75
800	.80
1000	.85
1250	.84
1600	.85
2000	.82
2500	.86
3150	1.05
4000	1.08
5000	.89
6300	1.18

MATERIALE : Type I6

Lydabsorberende skjerm type EP fra Hedemora.

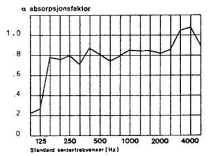

MÅLEBESKRIVELSE :

——— = 8 cm skjerm type EP med ensidig lydabsorbent.

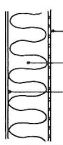

perforert stålplate

8 cm mineralullplate

0.7 mm stålplate

I 6

AKUSTISK LABORATORIUM
TILSLUTTET SINTEF
NORGES TEKNISKE HØGSKOLE
TRONDHEIM

ABSORPSJONSFAKTORER målt i klangrom
(ISO R354)

Hz	A
63	
80	
100	.35
125	.32
160	.47
200	.68
250	1.22
315	1.76
400	1.60
500	2.32
630	2.00
800	2.00
1000	1.85
1250	1.89
1600	1.71
2000	1.82
2500	1.67
3150	1.80
4000	
5000	
6300	

MATERIALE : Type I8

Skjermvegg type Systemvegg fra NOBØ

A, ekvivalent absorpsjonsareale, m^2 Sabin/m^2 skjerm

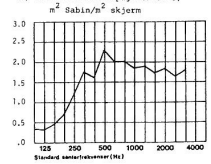

MÅLEBESKRIVELSE :

——— = målt med skjermene vilkårlig fordelt på betong gulvflate.
Skjermdimensjon:
1175 x 1420 x 82 mm

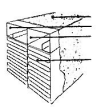

tekstil
stålramme
0.55 mm stålplate
4 cm mineralull
50 kg/m^3

I 8

AKUSTISK LABORATORIUM
TILSLUTTET SINTEF
NORGES TEKNISKE HØGSKOLE
TRONDHEIM

ABSORPSJONSFAKTORER målt i klangrom
(ISO R354)

Hz	α_1	α_2
63	.16	.24
80	.12	.23
100	.17	.23
125	.16	.26
160	.39	.52
200	.47	.47
250	.65	.57
315	.76	.75
400	.93	.76
500	.83	.79
630	.78	.69
800	.80	.76
1000	.85	.84
1250	.80	.77
1600	.81	.89
2000	.80	.89
2500	.90	.89
3150	.90	.91
4000	.88	.96
5000	.92	.98
6300	.96	1.02

MATERIALE : Type I9

Skjermvegg type Perfovegg fra Perfoverken AB.

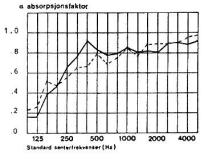

MÅLEBESKRIVELSE :

Produkt: Veggelement av 1 mm stålplater med mellomliggende 50 mm mineralullmatte. Bredde 600 mm, høyde inntil 3000 mm. Leveres med én eller begge sider perforert. Takelementer, veggelementer med vindu og dør leveres for innebygging av støykilder e.l.

——— = 50 mm tykt element, én side perforert (3 mm hull)
------- = 50 mm tykt element, begge sider perforert (3 mm hull)

Målt montert i veggåpning mellom to målerom.

I 9

AKUSTISK LABORATORIUM
TILSLUTTET SINTEF
NORGES TEKNISKE HØGSKOLE
TRONDHEIM

ABSORPSJONSFAKTORER målt i klangrom
(ISO R354)

Hz	α_1	α_2
63		
80		
100	.25	.39
125	.35	.56
160	.41	.58
200	.49	.52
250	.67	.65
315	.81	.69
400	.94	.82
500	.95	.72
630	.74	.65
800	.81	.75
1000	.87	.90
1250	.84	.78
1600	.82	.80
2000	.84	.86
2500	.87	.96
3150	.91	.97
4000	1.01	.90
5000	.96	1.03
6300		

MATERIALE : Type I11

Industristøyskjerm
type Q - Industrisystem
(Verkstads AB Lindqvist, Motala)

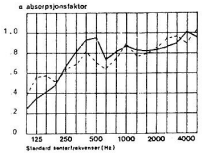

MÅLEBESKRIVELSE :

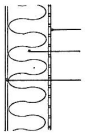

——— = én side av skjerm perforert, innlegg av 4 cm Stapelfiberskiva 363.

------ = begge sider av skjerm perforert, innlegg av 4 cm Stapelfiberskiva 359.

Skjermstørrelse : 190 cm x 83 cm.

Veggelementer er montert i veggåpning mellom to klangrom, med tilnærmet uendelig stort rom bak absorbent. Prøveareal : 6,9 m² .

I 11

AKUSTISK LABORATORIUM
TILSLUTTET SINTEF
NORGES TEKNISKE HØGSKOLE
TRONDHEIM

ABSORPSJONSFAKTORER målt i klangrom
(ISO R354)

Hz	α_1	α_2
63	.20	.23
80	.25	.16
100	.20	.27
125	.57	.21
160	.59	.56
200	.68	.52
250	.81	.64
315	.85	.78
400	.78	.82
500	.83	.77
630	.68	.67
800	.77	.72
1000	.80	.84
1250	.82	.81
1600	.85	.99
2000	.81	.86
2500	.91	.99
3150	.93	1.05
4000	.95	.86
5000	.99	.93
6300	1.03	1.04

MATERIALE : Type I10

Skjermvegg type Perfovegg fra Perfoverken AB.

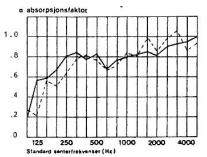

MÅLEBESKRIVELSE :

Produkt: veggelement av 1 mm stålplater med mellomliggende 100 mm mineralullmatte. Bredde 600 mm, høyde inntil 3000 mm. Leveres med én eller begge sider perforert. Takelementer, veggelementer med vinduer og dør leveres for innbygging av støykilder e.l.

——— = 100 mm element, én side perforert (3 mm hull)

------ = 100 mm element, begge sider perforert (3 mm hull)

Målt montert i veggåpning mellom to målerom.

I 10

AKUSTISK LABORATORIUM
TILSLUTTET SINTEF
NORGES TEKNISKE HØGSKOLE
TRONDHEIM

ABSORPSJONSFAKTORER målt i klangrom
(ISO R354)

Hz	α_1	α_2	α_3
63	.10	.15	.30
80			
100			
125	.30	.30	.50
160			
200			
250	.65	.70	.80
315			
400			
500	.85	.85	1.00
630			
800			
1000	.90	.90	1.00
1250			
1600			
2000	.90	.90	1.00
2500			
3150			
4000	.90	.85	1.00
5000			
6300			

MATERIALE : Type I12

Skjerm-element
type Rockfon Inbyggnadselement fra Rockwool

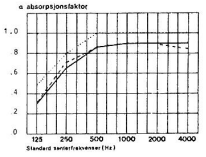

MÅLEBESKRIVELSE :

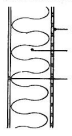

Standardelement :
579 mm x 2500 mm og
1179 mm x 2500 mm

——— = veggelement med 40 % perforert plate på én side.

- - - - - = veggelement med 23 % perforert plate på én side

····· = takelement med 20 cm mineralullplate i SB-beresystem.

Elementene er montert i prøveåpning for vegger mellom to klangrom, med tilnærmet uendelig stort rom på én side.

I 12

AKUSTISK LABORATORIUM
TILSLUTTET SINTEF
NORGES TEKNISKE HØGSKOLE
TRONDHEIM

ABSORPSJONSFAKTORER malt i klangrom
(ISO R354)

Hz	A
63	
80	
100	.27
125	.51
160	.53
200	.61
250	.51
315	.81
400	.98
500	.94
630	1.17
800	1.31
1000	1.26
1250	1.33
1600	1.33
2000	1.25
2500	1.14
3150	1.08
4000	1.01
5000	1.08
6300	

MATERIALE : Type I13

SKJERMVEGG.

A, ekvivalent absorpsjonsareale,
m^2 Sabin/m^2 skjerm

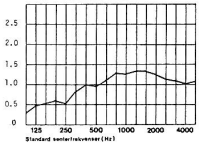

MÅLEBESKRIVELSE :

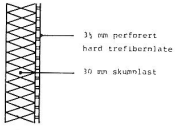

5 stk. skjermer á 1650 mm x 900 mm vilkårlig fordelt på gulvflaten i klangrom

Spesialskjerm for Norsk Rikskringkasting

I 13

AKUSTISK LABORATORIUM
TILSLUTTET SINTEF
NORGES TEKNISKE HØGSKOLE
TRONDHEIM

ABSORPSJONSFAKTORER malt i klangrom
(ISO R354)

Hz	α
63	
80	
100	.14
125	.29
160	.15
200	.19
250	.24
315	.33
400	.49
500	.63
630	.96
800	1.15
1000	1.28
1250	1.36
1600	1.56
2000	1.74
2500	1.79
3150	1.84
4000	1.80
5000	1.76
6300	

MATERIALE : Type I14

Skjermvegg fra Stål og Stil A/S.

A, ekvivalent absorpsjonsareale,
m^2 Sabin/m^2 skjerm.

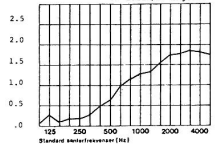

MÅLEBESKRIVELSE :

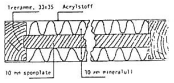

— målt med skjermene plassert på en rett linje, diagonalt over gulvflaten.

Skjermdimensjon:
35 x 900 x 1280 mm.

I 14

D.6 Measurement uncertainties

Measurement uncertainty

From a world wide Round Robin[1)], in which SP took part, with 23 participating laboratories from 11 countries, the following measurement uncertainty has been calculated

Frequencies	
(Hz)	**Uncertainty**
100-630	± 0,15
800-1250	± 0,10
1600-2500	± 0,15
3150-5000	± 0,20

[1)] The figures are calculated from twice the standard deviations, rounded to the nearest 0,05. The data from the Round Robin is documented in a letter from the ASTM to the participating laboratories.

Figure 11: Measurement uncertainties from Daniela T. Helboe [17].